# A Tour of My Research on laser-based molecular spectroscopy

許艷珠 Yen-Chu Hsu
中央大學物理系
專案研究員
Lab:305室

# The Electromagnetic spectrum

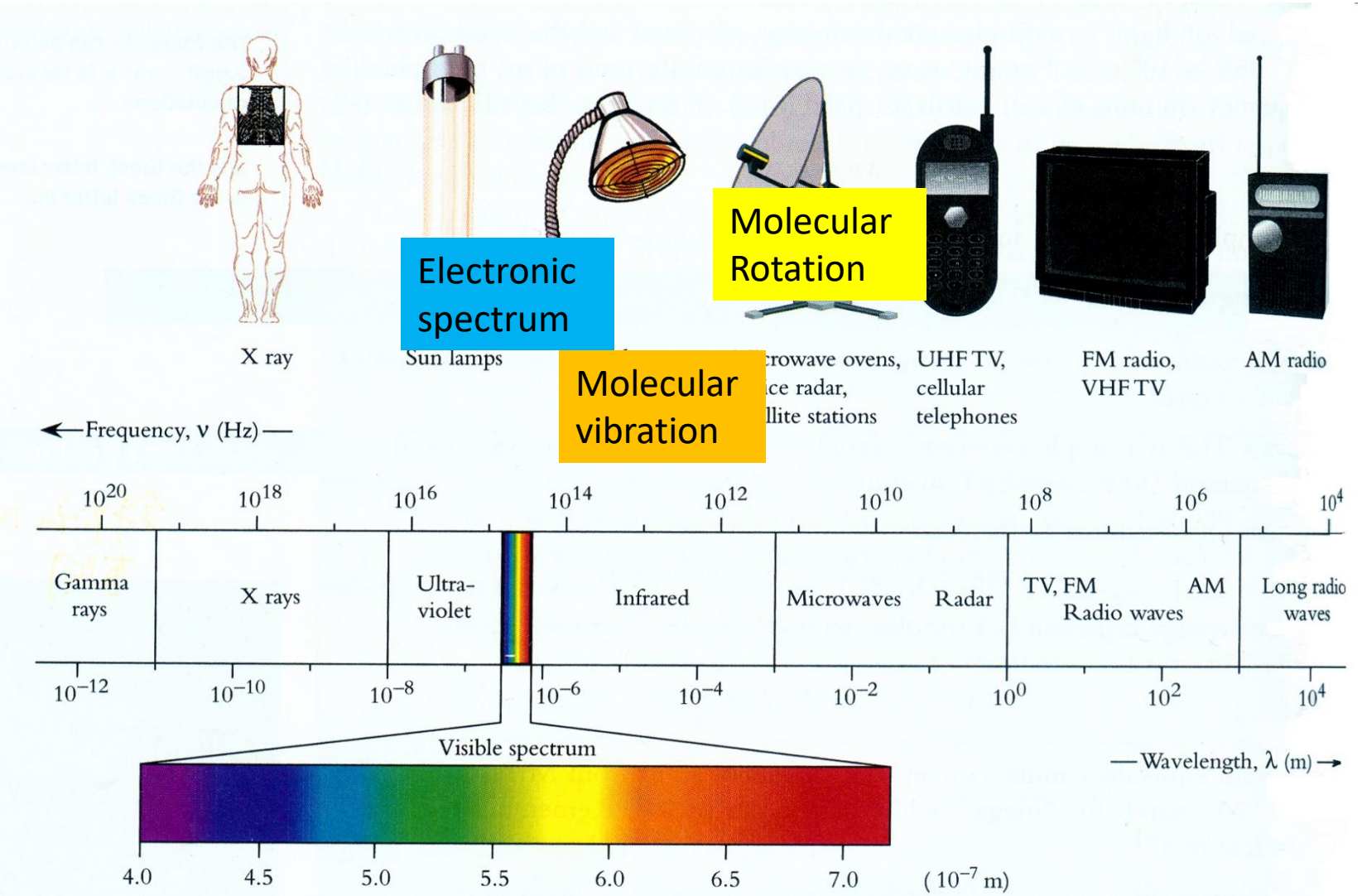

# The Born-Oppenheimer Approximation

The full molecular Hamiltonian is

$$\hat{\mathcal{H}} = \underbrace{\frac{1}{2m_e}\sum_e p_e^2}_{\text{Electron KE}} + \underbrace{\frac{1}{2}\sum_n \frac{P_n^2}{M_n}}_{\text{Nuclear KE}} + \underbrace{V(q_e, Q_n)}_{\substack{\text{Electrostatic} \\ \text{interactions} \\ \text{between the} \\ \text{charged particles}}}$$

The Schrödinger equation is

$$\hat{\mathcal{H}}\Psi_{evr}(q_e, Q_n) = E\Psi_{evr}(q_e, Q_n)$$

In the Born-Oppenheimer approximation we assume that electrons, being lighter and faster than nuclei, adapt instantly to the configuration of the nuclei, and take up one of their stationary states. This is equivalent to writing the wavefunctions as products of electron and nuclear parts, i.e

$$\Psi_{evr}(q_e, Q_n) = \sum_i \psi_{ei}(q_e, Q_n) \cdot \psi_{vr}^{(i)}(Q_n)$$

$\psi_e(q_e, Q_n)$ is a solution of the electron Schrödinger equation, for which the Hamiltonian is

$$\hat{H}_e = \frac{1}{2m_e}\sum_e p_e^2 + \hat{V}(q_e, Q_n).$$

# Nuclear motion follows the following equation

$$\left(\frac{1}{2}\sum_n \frac{P_n^2}{M_n} + \right.$$

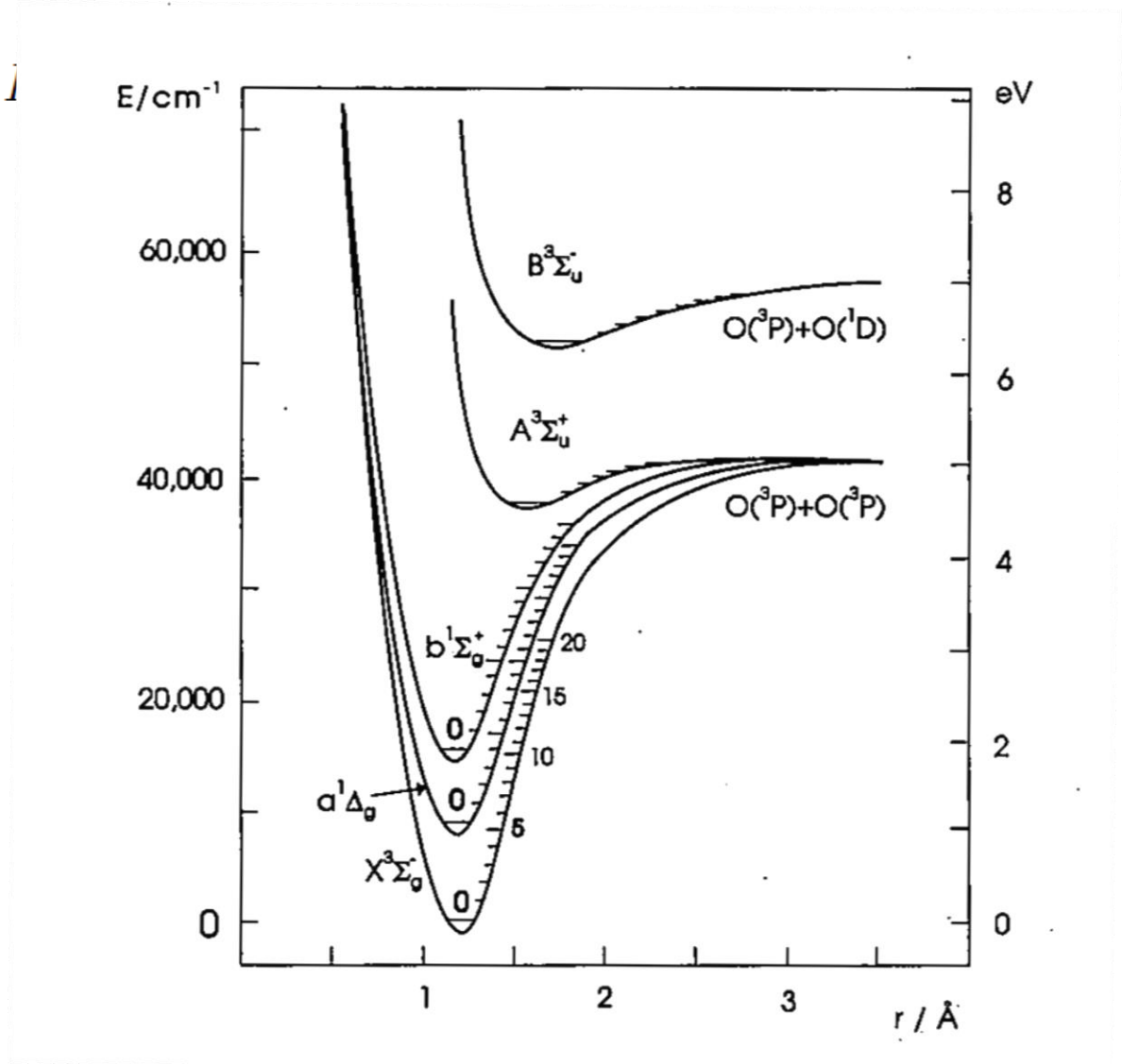

# Degrees of freedom of a molecule

Translation: 3, Rotation: 3 (non-linear molecule), Vibration: **3N-6**
2 (linear molecule) , Vibration: **3N-5**

## Nornal Modes of water

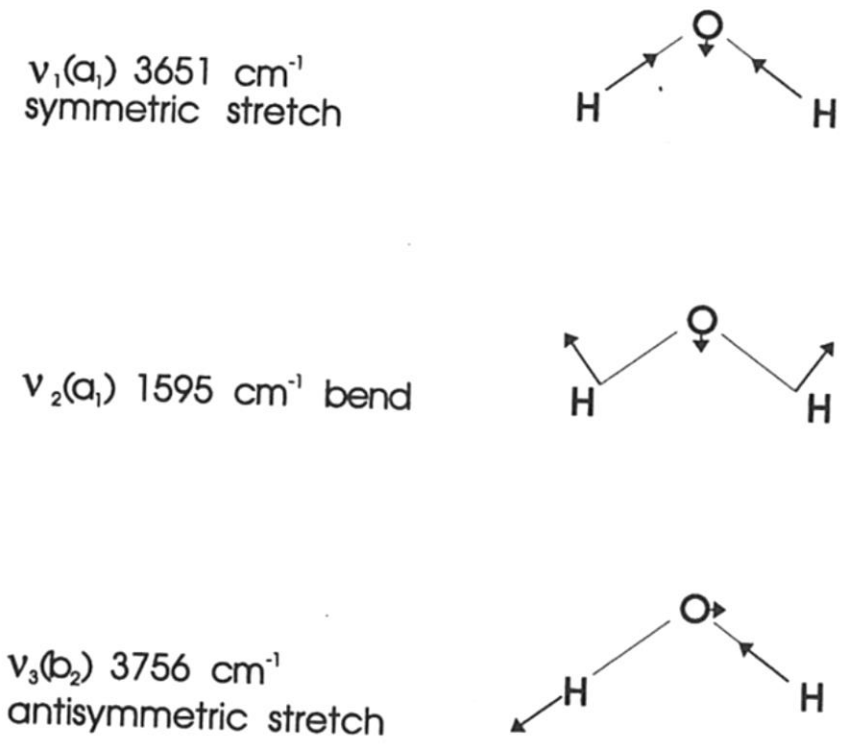


**Figure 7.58.** The normal vibrational modes of $H_2O$.

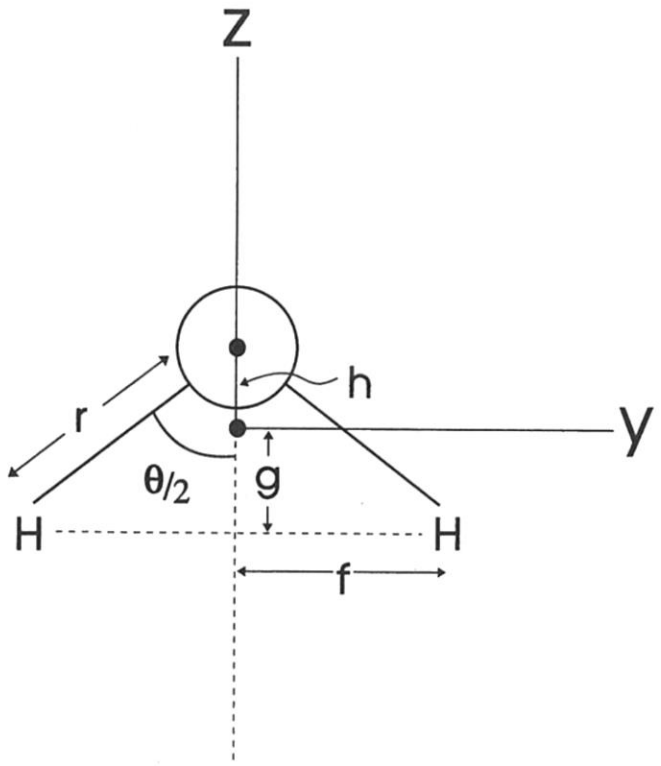


**Figure 6.5.** The $H_2O$ molecule.

# Rotational Spectroscopy

Energy level:

A, B, C :moments of inertia

Diatomic and linear molecule

$G(J)= B\vec{R}\bullet\vec{R}= B(\vec{J}-\vec{L}-\vec{S})^2=B[J(J+1)-\Omega^2]+DJ^2(J+1)^2$

Nonlinear molecule

$A\geq B \geq C$

B=C or A=B  Prolate/Oblate symmetric top

$G(J, K)=BJ(J+1)-(A-B)K^2$

$A\neq B\neq C$  asymmetric top

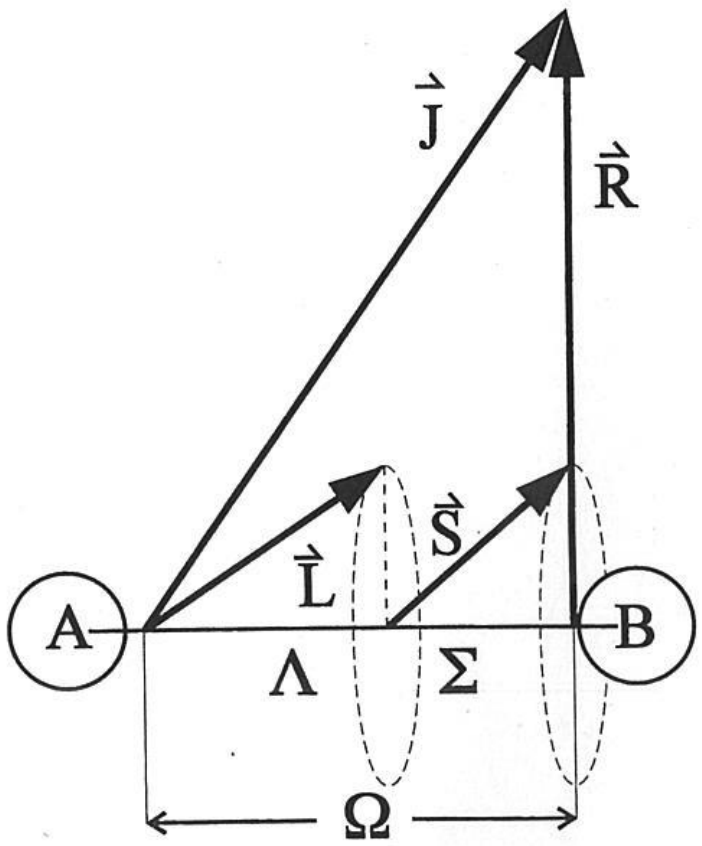


gure 9.3. Angular momenta in a diatomic molecule.

Selection Rules

$\mu \neq 0, \Delta J = 0, \pm 1, \Delta K = 0, \pm 1$

# Vibrational Spectroscopy

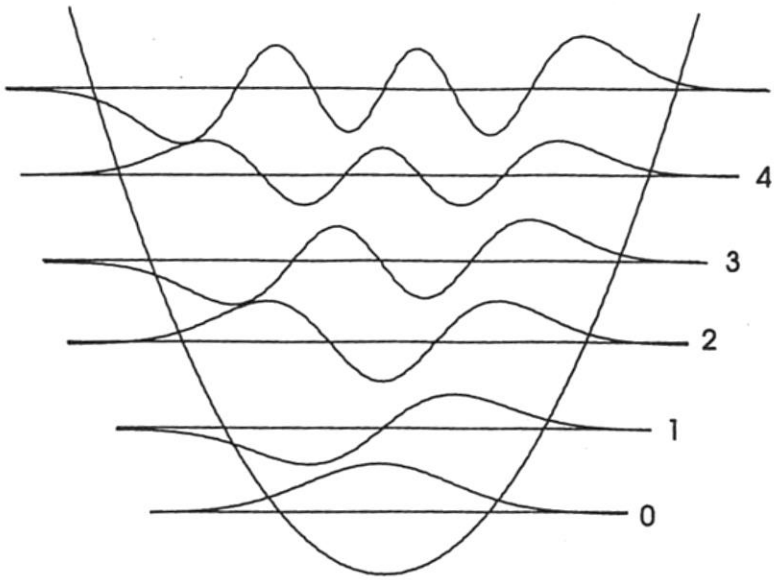


**Figure 7.3.** The harmonic oscillator wavefunctions.

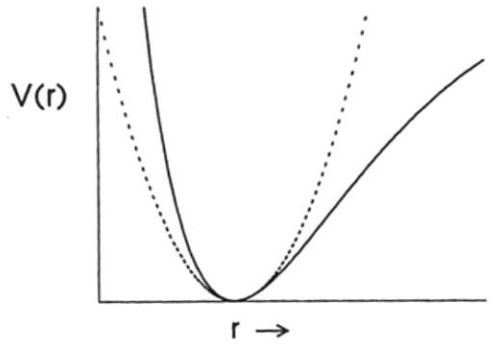


**Figure 7.4.** A harmonic oscillator potential (dots) as compared to a realistic diatomic potential (solid).

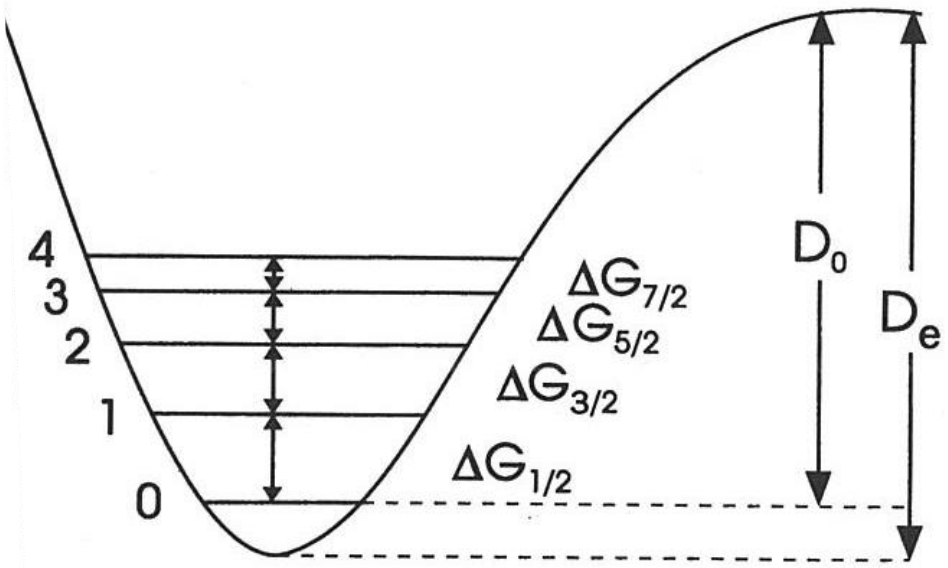


**7.8.** The vibrational intervals of a diatomic molecule.

# Vibrational Energy And Selection Rules

$$G(v_1, v_2, \ldots v_i \ldots) = \sum_i^{3N-5(6)} \omega_{ei} \left(v_i + \frac{1}{2}\right) + \sum_{i \le j}^{3N-5(6)} x_{ij} \left(v_i + \frac{1}{2}\right)\left(v_j + \frac{1}{2}\right) + \sum_{i \le j}^{3N-5(6)} g_{ij} l_i l_j$$

Pure vibration-rotational transition

$\partial\mu/\partial x \neq 0$, $\mu$: dipole moment, $x$: vibrational coordinate

$\Delta v_i = \pm 1$

# Selection Rules of Electronic band

- $< \boldsymbol{f}|\hat{\mu}|\boldsymbol{i} > \neq \mathbf{0}$
- $< v_f| v_i > \neq 0$

  Franck-Condon Factor:

  $< \mathbf{v_f}| \mathbf{v_i} >^2$
- **Total Pariety**

  $+ \leftrightarrow -$
- $\Delta S=0$
- $\Sigma^+ \leftrightarrow \Sigma^+, \Sigma^- \leftrightarrow \Sigma^-$
- **Selection rules of angular momentum**

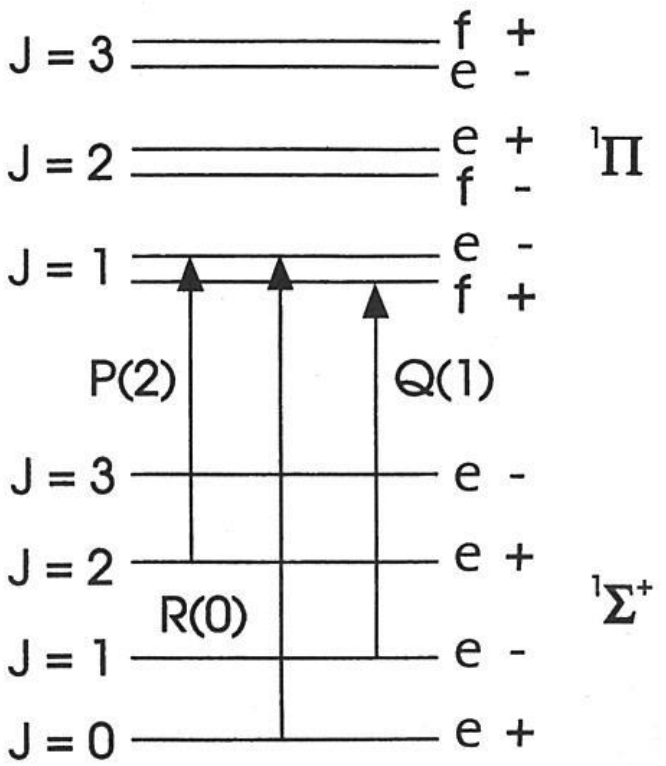


**7.33.** Energy-level diagram for a $\Pi$–$\Sigma$ transition.

# How to analyze a spectrum?

## Combination difference

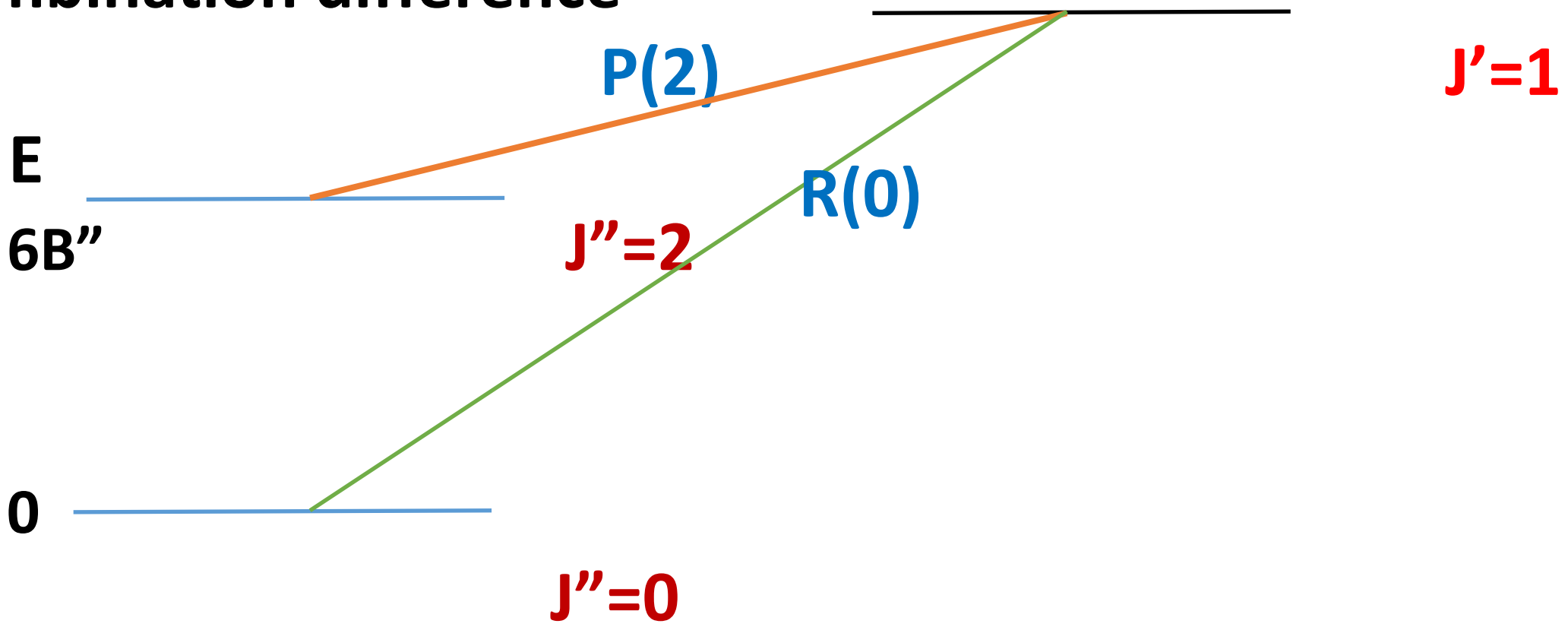


## Basic concepts

Harmonic oscillators and Rigid Rotors

Perturbation theory and effective Hamiltonian

# Laser spectroscopic studies of ScC radical in our laboratory

1. C.W. Chen, A. J. Merer, and Yen-Chu Hsu, J. Chem. Phys. **149**, 074302-1-074302-15 (2018).

2. C.W. Chen, A. J. Merer, and Yen-Chu Hsu, J. Mol. Spectrosc. **361**, 40-46(2019).

# Laser Ablation of Metal Rod

Metastable Sc atoms generated by 532nm-laser ablation of a rotating Sc rod were reacted with $CH_4$ or $C_2H_2$ seeded in Ar or He under supersonic beam conditions. A Nd:Yag pumped dye laser was used to probe the products by laser-induced.

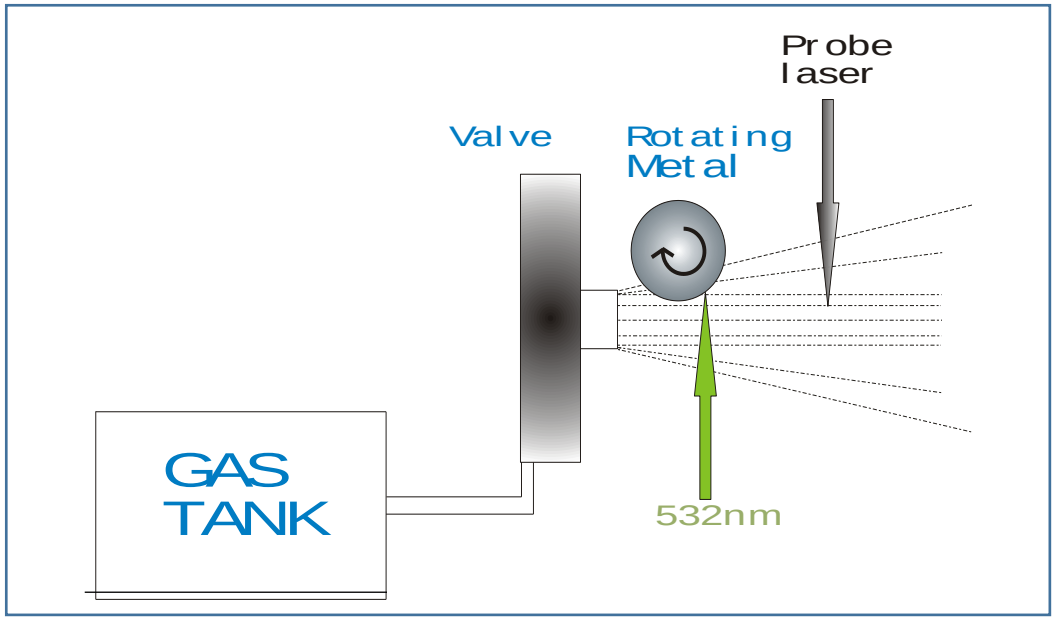

# Laser Ablation setup

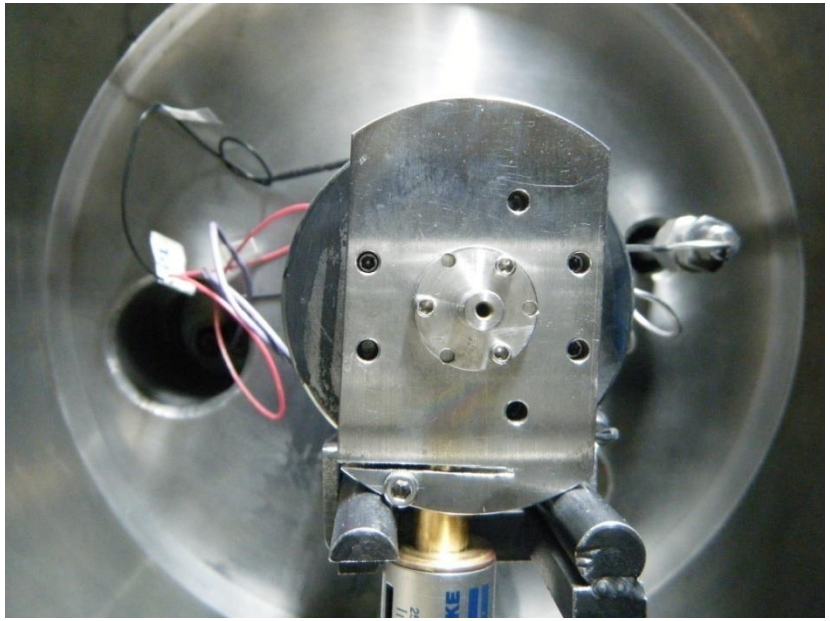

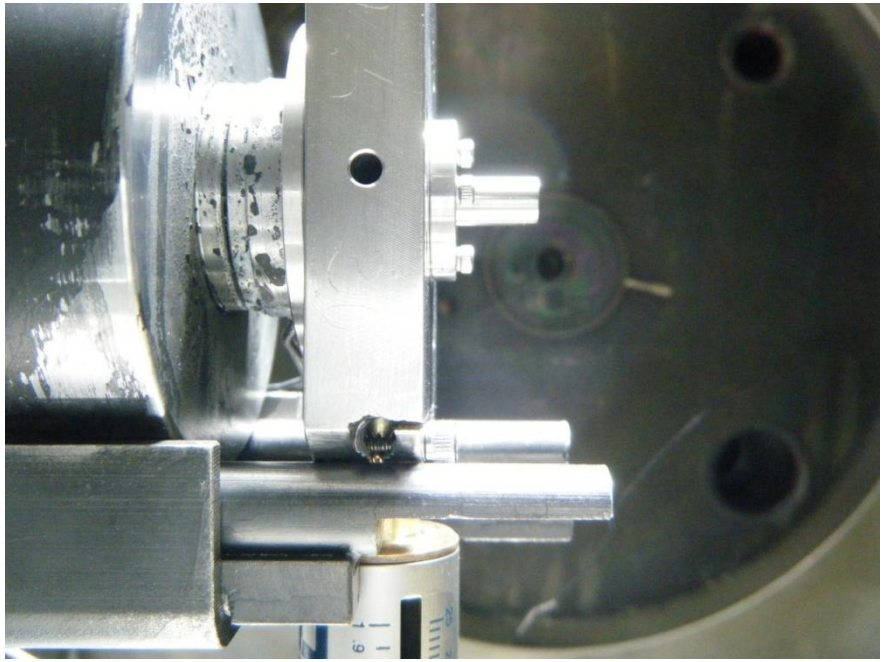

# Introduction of Metal Carbides

- Sc atom is the least abundant of the 3*d transition metals* in the Earth's crust.
- *Scandium oxide, ScO*, gives comparatively intense band systems in the spectra of cool M-type stars.
  With carbon and oxygen having comparable cosmic abundances, *ScC* is a molecule of possible astrophysical significance.
- *ScC and MnC* are the only remaining 3*d transition metals monocarbides that have not been characterized.*

$Sc^{13}C$: $\Omega=5/2 - 3/2$
band at 14640 $cm^{-1}$

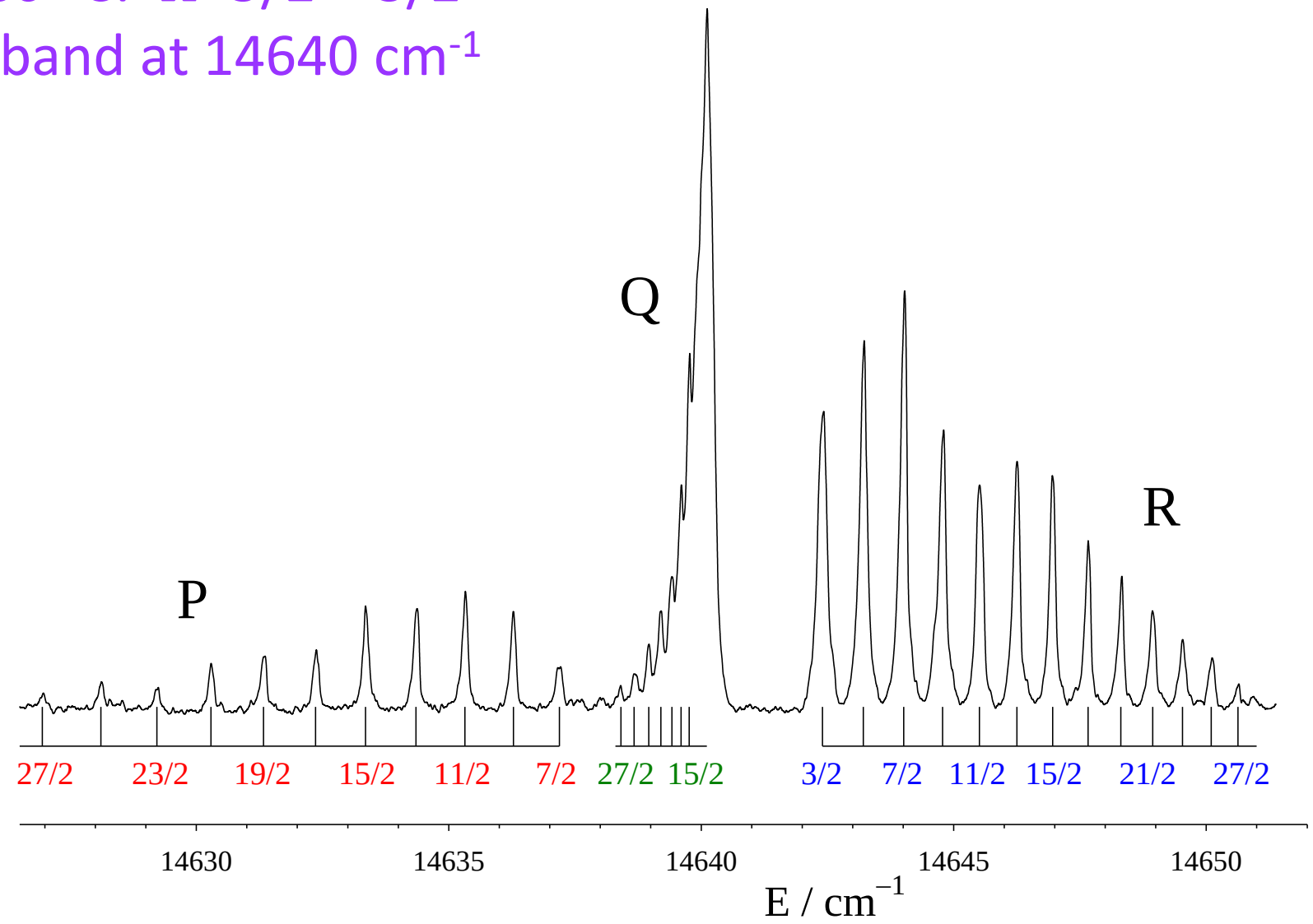

# ScC; the 15521 $cm^{-1}$ bands

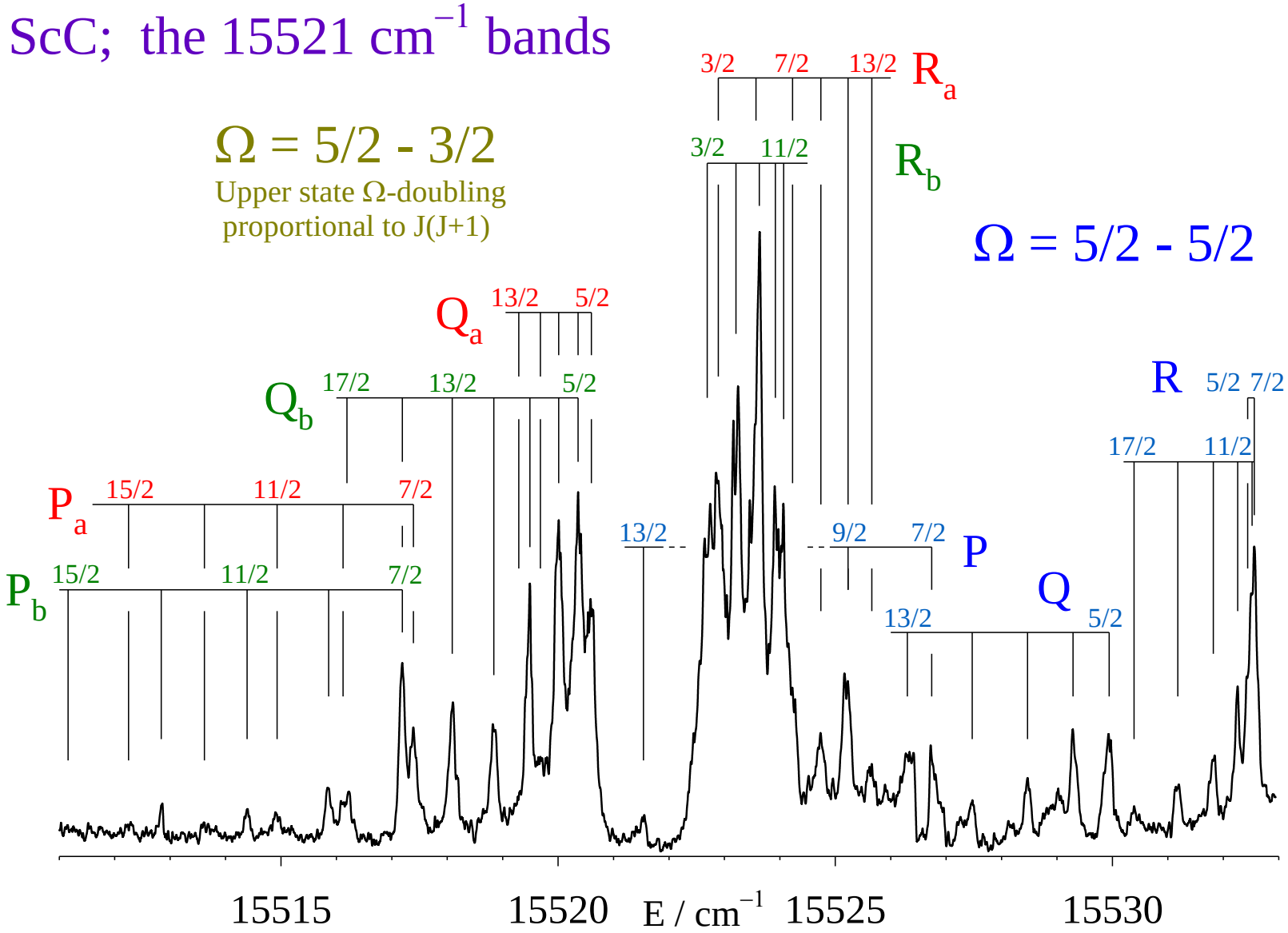

# Absorption and Emission

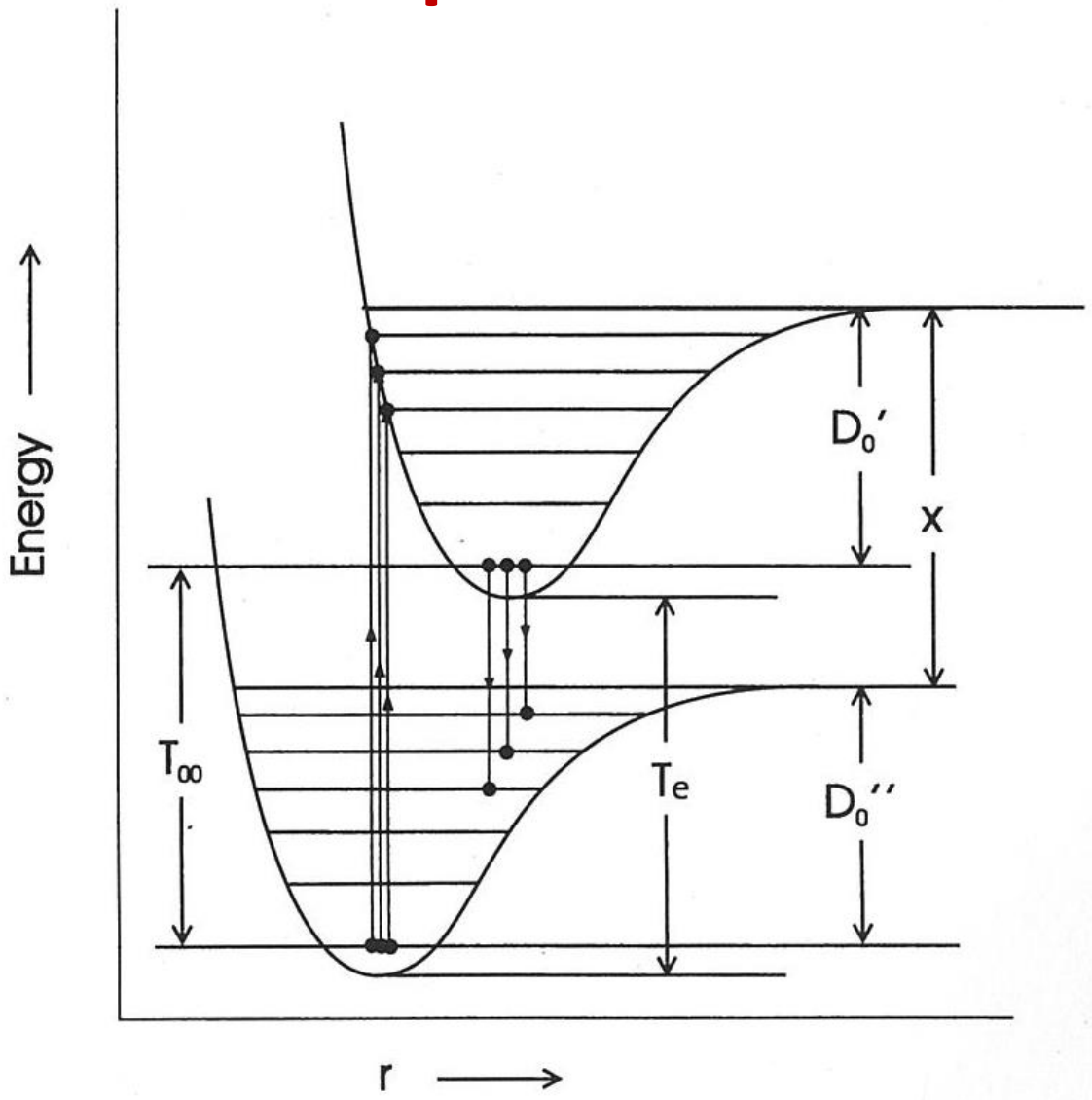


**Figure 9.27.** Absorption and emission progressions.

# Emission from the $\Omega$=5/2 – $X^2\Pi_{3/2}$ band at 15521 $cm^{-1}$

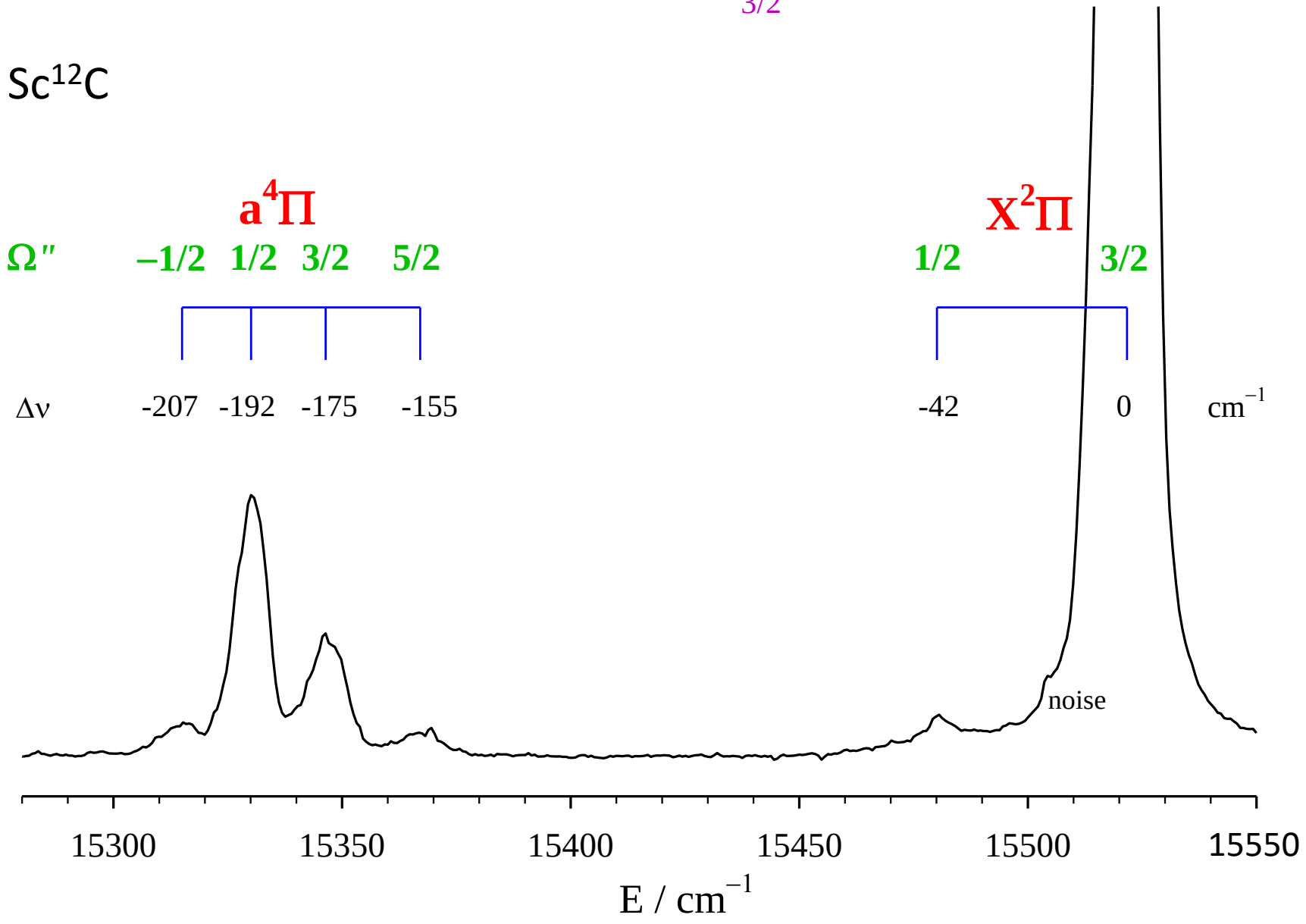

# Emission spectra from selected bands of $Sc^{12}C$

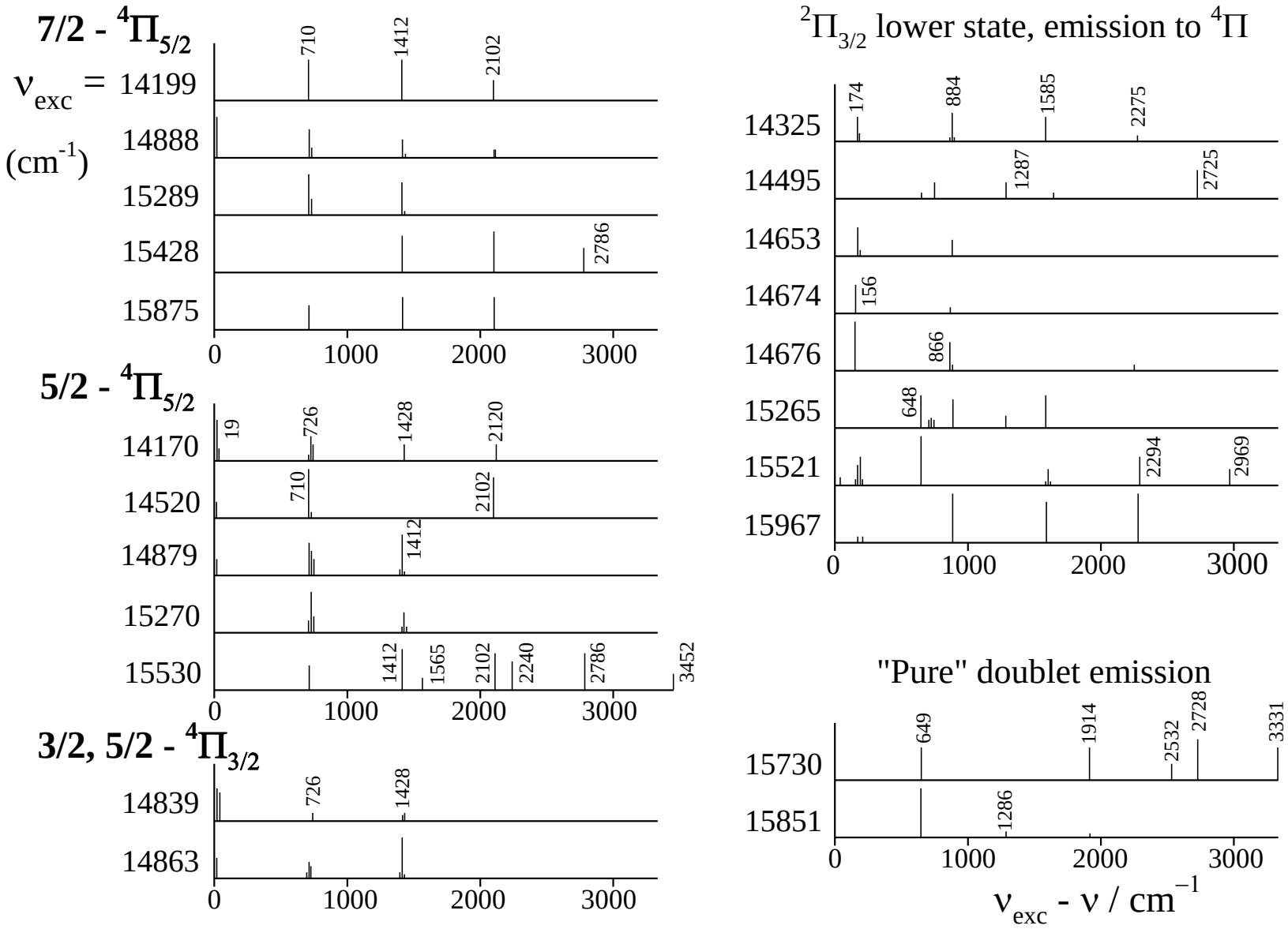

# $Sc^{12}C$: low-lying spin and vibrational levels

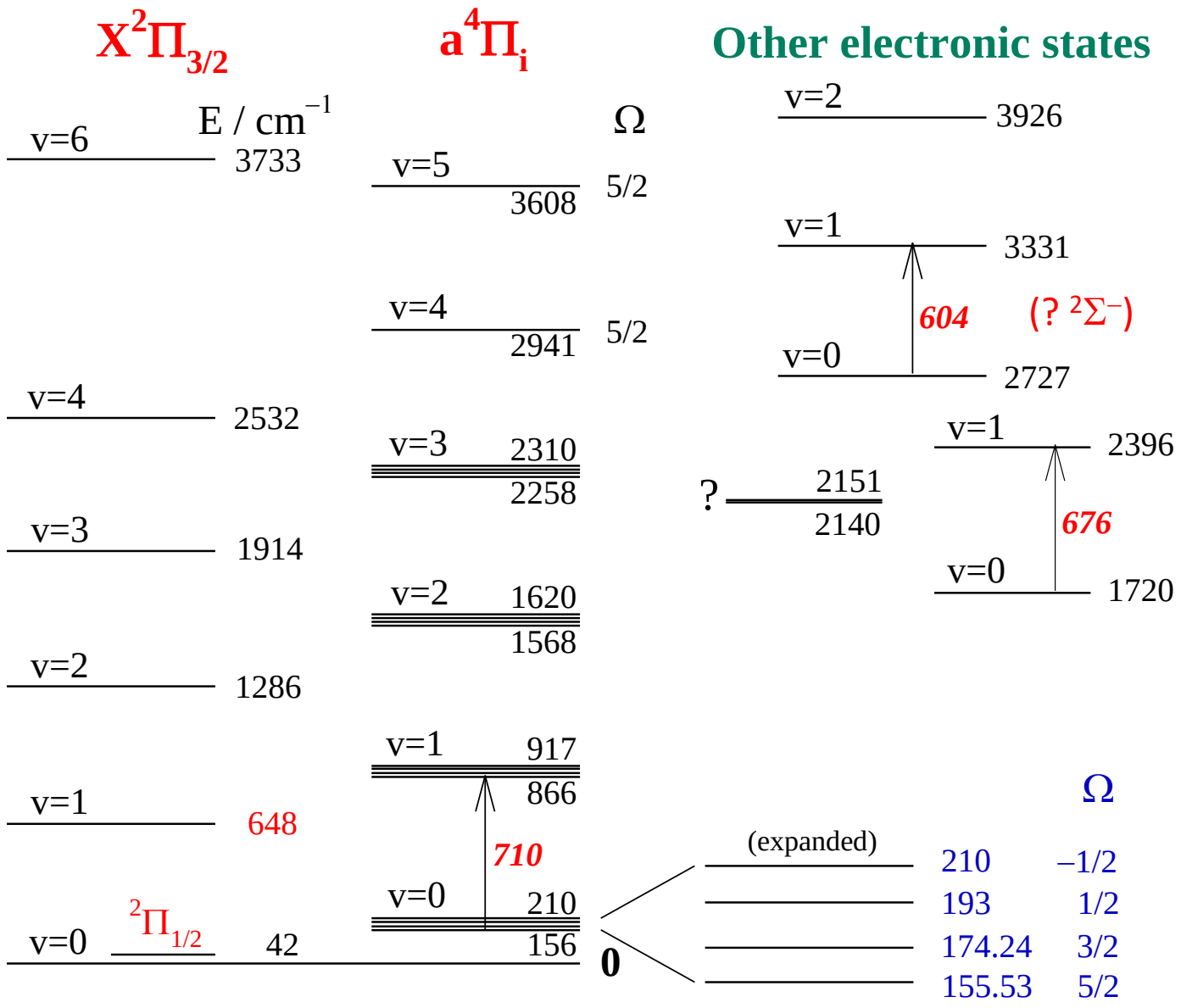

# $Sc^{13}C$: perturbation in the 15028 $cm^{-1}$ level

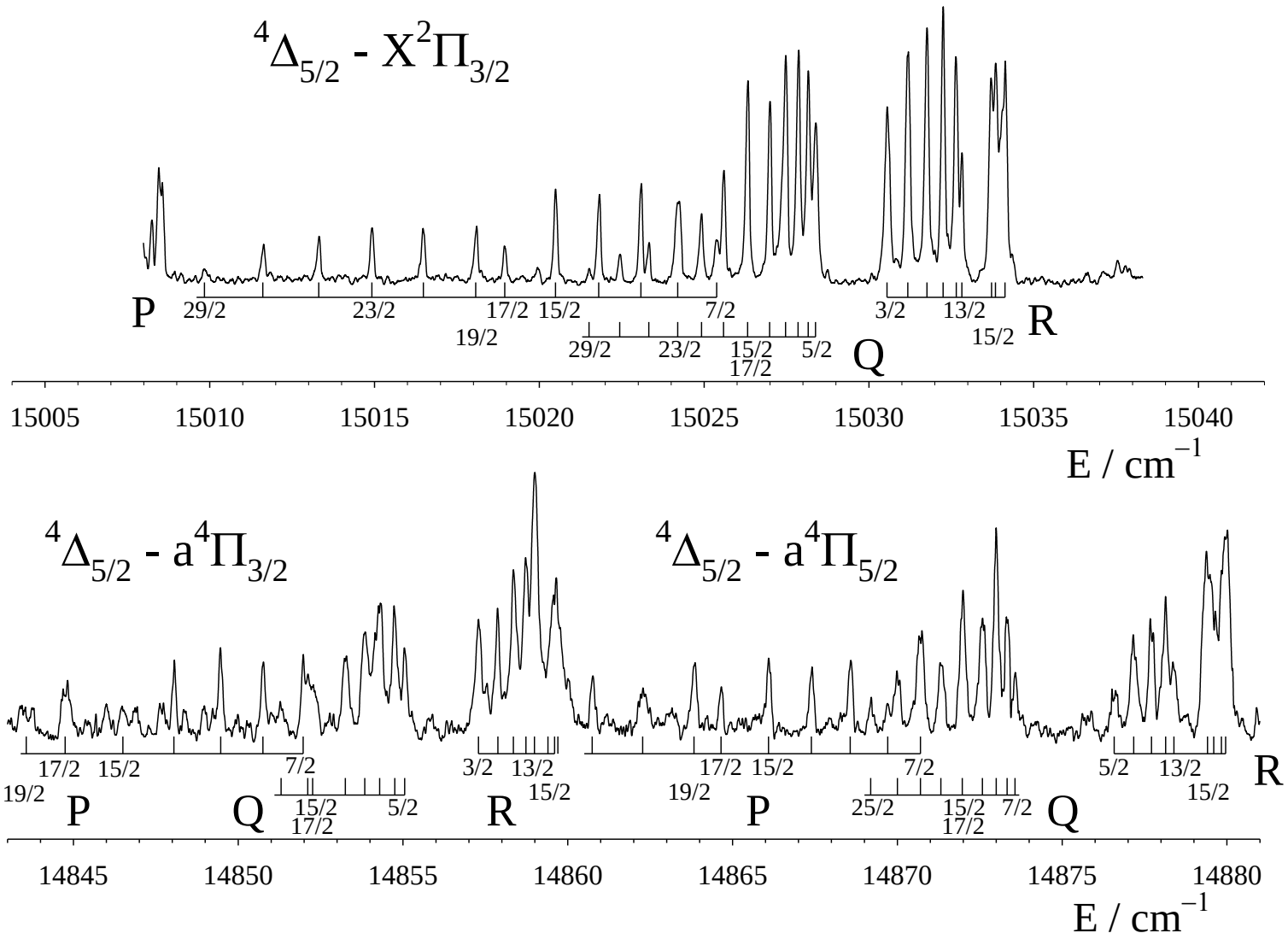

**Rotational constants for the $X^2\Pi$, $a^4\Pi_{5/2}$ and $a^4\Pi_{3/2}$ states of $Sc^{12}C$ and $Sc^{13}C$. Values in $cm^{-1}$. Quoted error limits are $3\sigma$.**

| | | $Sc^{12}C$ | $Sc^{13}C$ |
|---|---|---|---|
| $X^2\Pi_{3/2}$ | $T_0$ | 0 | 0 |
| | B | $0.4616_7 \pm 0.0003_9$ | $0.4341_7 \pm 0.0004_0$ |
| | $10^7D$ | 9.4 fixed | 8.2 fixed |
| $X^2\Pi_{1/2}$ | $T_0$ | $39.46_9 \pm 0.01_8$ | $39.31_8 \pm 0.02_3$ |
| | B | $0.4724_5 \pm 0.0012_3$ | $0.4418_4 \pm 0.0011_5$ |
| | $10^7D$ | 0 fixed | 0 fixed |
| $a^4\Pi_{5/2}$ | $T_0$ | $155.58_4 \pm 0.02_6$ | $154.71_7 \pm 0.02_8$ |
| | B | $0.4534_7 \pm 0.0009_5$ | $0.4278_9 \pm 0.0009_5$ |
| | $10^4D$ | $-0.19_8 \pm 0.07_0$ | $-0.15_0 \pm 0.08_0$ |
| $a^4\Pi_{3/2}$ | $T_0$ | $174.31_1 \pm 0.03_3$ | $173.24_2 \pm 0.03_6$ |
| | B | $0.4703_9 \pm 0.0018_6$ | $0.4447_0 \pm 0.0022_2$ |
| | $10^4D$ | $-0.34_3 \pm 0.21_6$ | $-0.20_8 \pm 0.30_4$ |
| | $\sigma$ | 0.017 | 0.018 |

$r_0 = 1.952(1)$ Å

$r_0 = 1.928(7)$ Å

# Bond lengths in the "early" 3d and 4d monocarbides

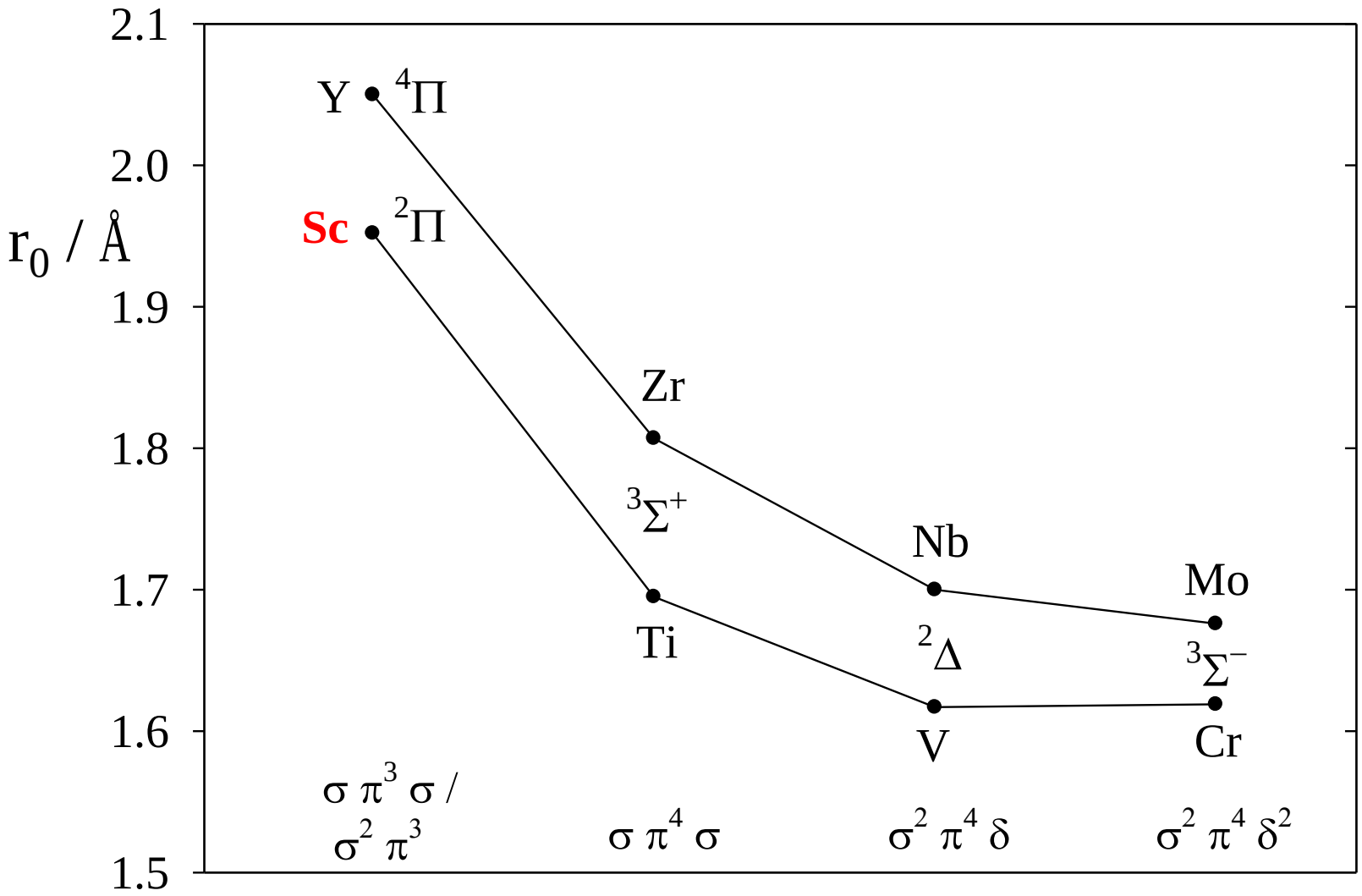

# Potential energy curves for ScC

Two *ab initio* calculations have been done:-

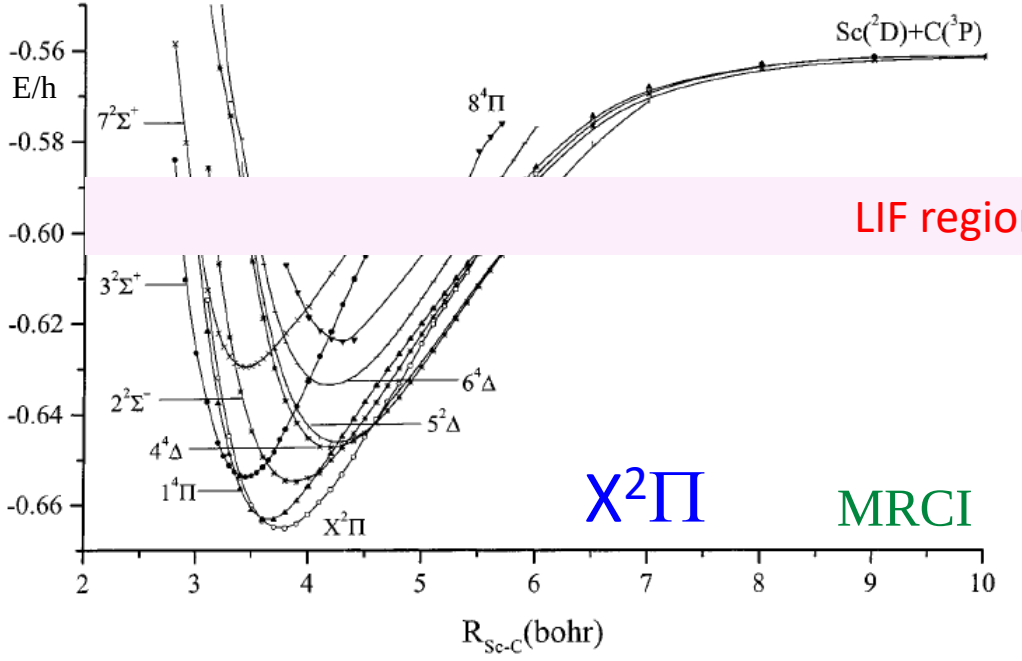


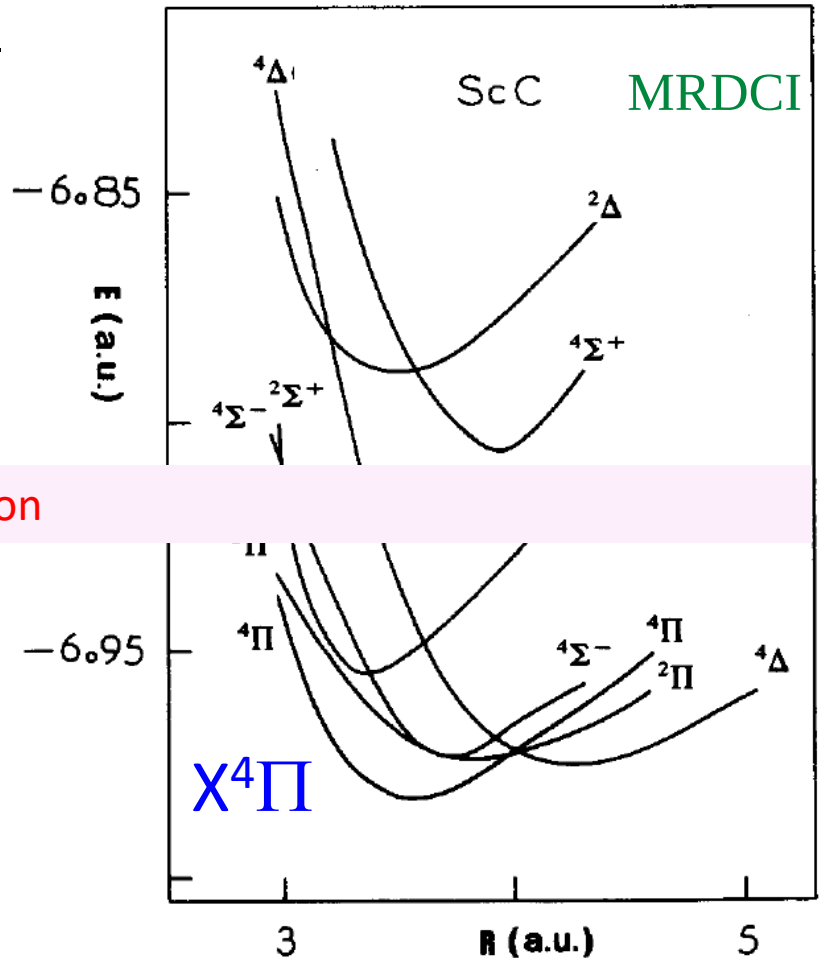


LIF region

A. Kalemos, A. Mavridis and J.F. Harrison,
J. Phys. Chem. A, **105,** 755 (2001)

G.H. Jeung and J. Koutecký,
J. Chem. Phys. **88**, 3747 (1988)

# The low-lying electronic states of ScC

The lowest observed state has $\Omega = 3/2$, consistent with $^2\Pi_i$ or $^2\Delta_r$. However no low-lying $^2\Delta_r$ states are expected.

We find it has $r_0 = 1.952(1)$ Å $\Delta G_{1/2} = 648$ cm$^{-1}$

Kalemos *et al* calculate $r_e = 1.973$ Å $\omega_e = 690$ cm$^{-1}$

---

A very low-lying $^4\Pi_i$ state has A = 18.7 cm$^{-1}$ (spin-orbit coupling).

We find $r_0 = 1.928(7)$ Å ; $\Delta G_{1/2} = 710$ cm$^{-1}$; $T_0 = 155$ cm$^{-1}$

Kalemos *et al*: $r_e = 1.937$ Å ; $\omega_e = 694$ cm$^{-1}$; $T_e = 432$ cm$^{-1}$

The

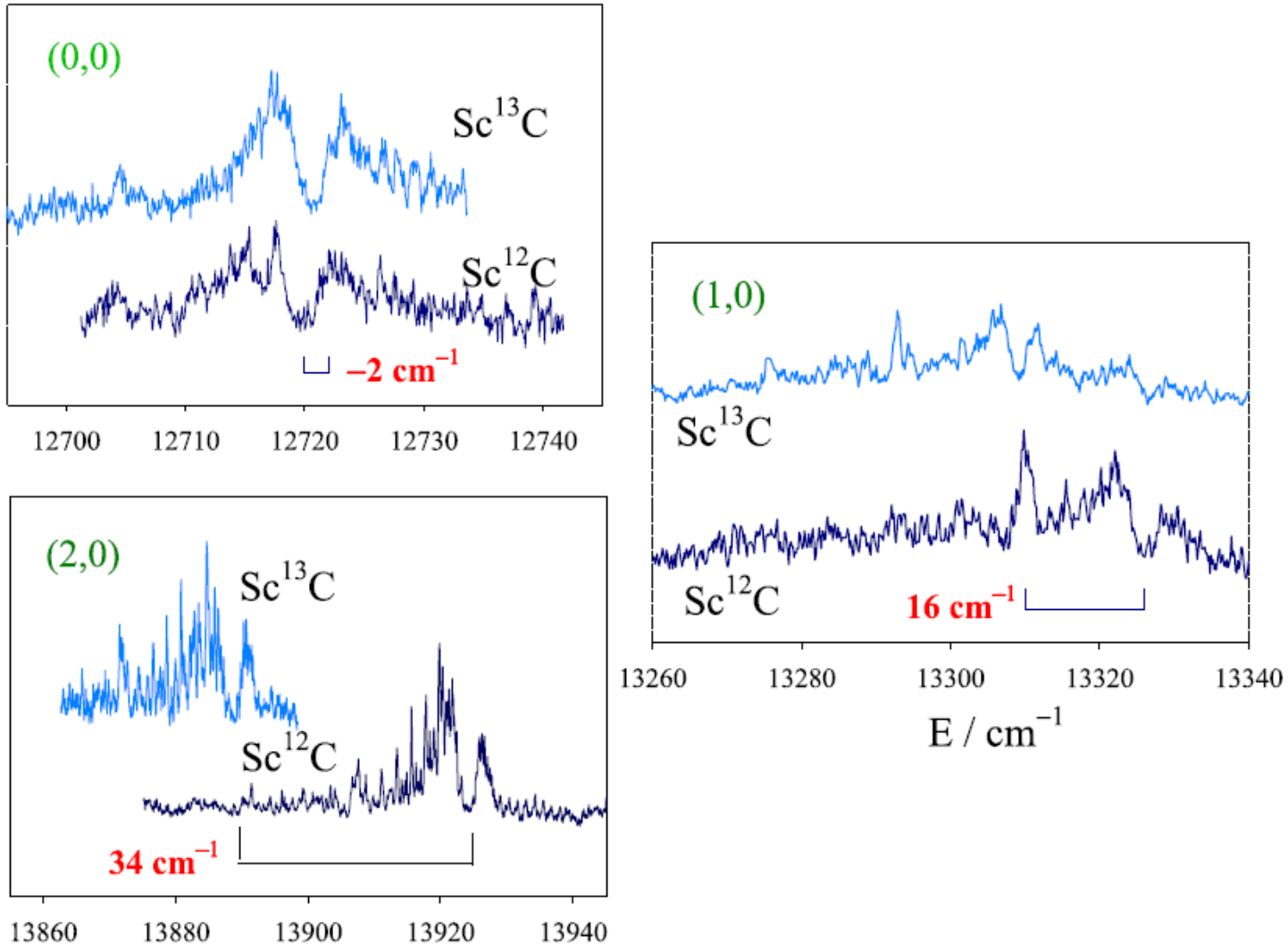


**Fig. 1.** The (0,0), (1,0) and (2,0) bands of the $^4\Sigma - a^4\Pi$ transitions of $Sc^{12}C$ and $Sc^{13}C$, illustrating their isotope shifts. The brackets point to the $^4\Sigma - {}^4\Pi_{5/2}$ sub-band origins, which are prominent dips in the rotational structure.

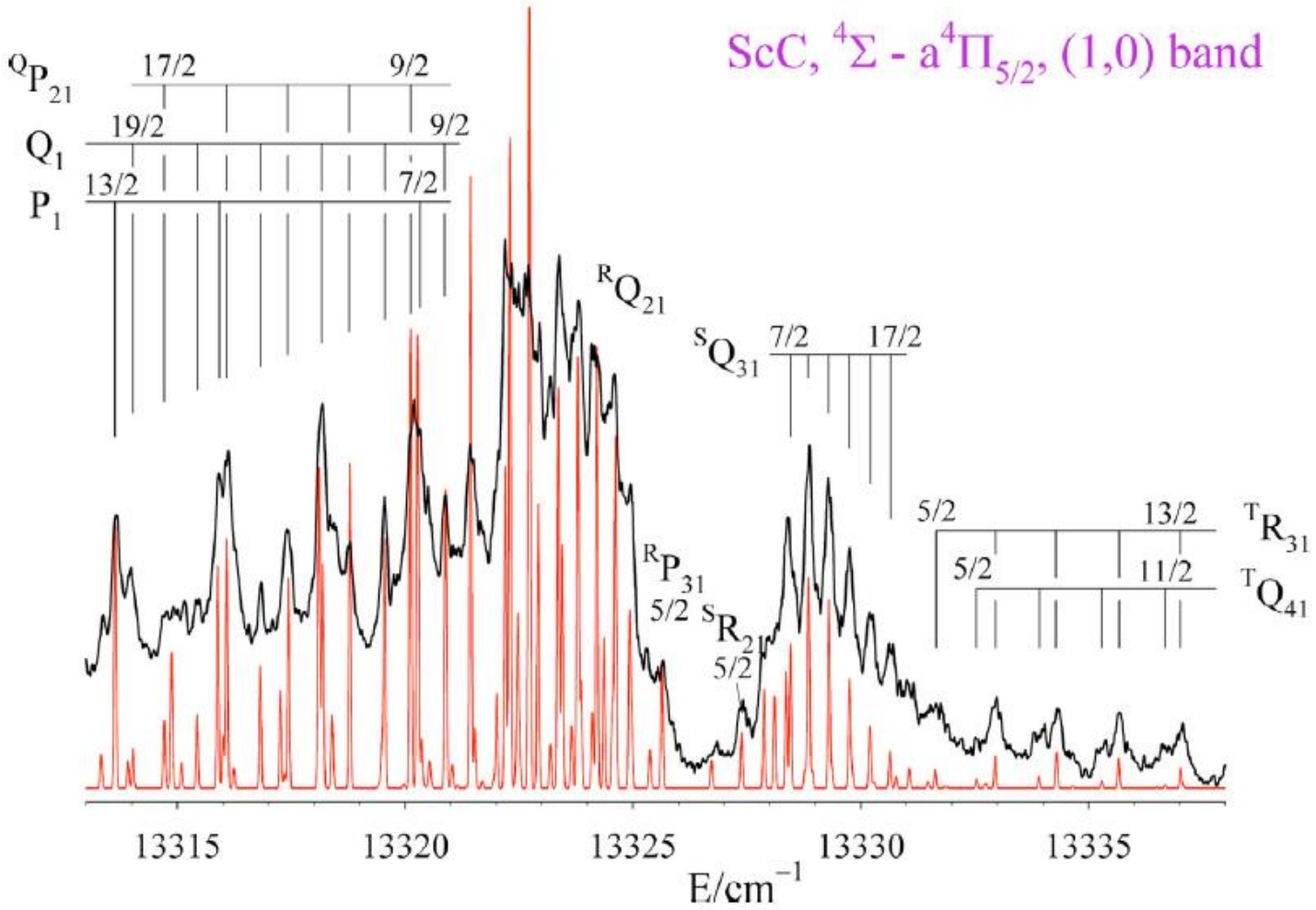


**Fig. 2.** The $Sc^{12}C$, $^4\Sigma - a^4\Pi_{5/2}$, (1,0) sub-band, with the assignments of six of the 12 branches marked. The band contour calculated from the final least squares results is also shown (colored red in the on-line version). The line width for the calculated contour is 0.1 $cm^{-1}$, which is narrower than the experimental line width in order to show the details of the rotational structure. A temperature of 16 K was assumed. (For interpretation of the references to colour in this figure legend, the reader is referred to the web version of this article.)

**Table 1**
Matrix elements for the spin and rotation of a $^4\Sigma^-$ electronic state.

| | $\|J, 1/2\ e/f\rangle$ | $\|J, 3/2\ e/f\rangle$ |
|---|---|---|
| $\langle J, 1/2\ e/f\|$ | $T_0 - 2\lambda - 7\gamma/2 + B(x+4)$ $- D\,[(x+4)^2 + 7x + 4]$ $\mp (2J+1)[B - \gamma/2 - 2D\,(x+4)]$ | symmetrical |
| $\langle J, 3/2\ e/f\|$ | $-\sqrt{3x}[B - \gamma/2 - 2D\,(x+2)$ $\pm 2D\,(J+1/2)]$ | $T_0 + 2\lambda - 3\gamma/2 + Bx$ $-D\,(x^2 + 3x)$ |

$x = J(J+1) - 3/4$.
For a $^4\Sigma^-$ state the $F_1$ and $F_3$ spin component levels correspond to the sum basis $2^{-1/2}\,[|J, \Omega\rangle + |J, -\Omega\rangle]$, and have *e* symmetry; the $F_2$ and $F_4$ levels (difference basis, $2^{-1/2}\,[|J, \Omega\rangle - |J, -\Omega\rangle]$) have *f* symmetry. The parameters $\lambda$ and $\gamma$ are the coefficients of the spin-spin and spin-rotation interactions, respectively.

**Table 2**
Matrix elements for the spin and rotation of a $^4\Pi$ electronic state.

| | $\lvert J, -1/2\ e/f\rangle$ | $\lvert J, 1/2\ e/f\rangle$ | $\lvert J, 3/2\ e/f\rangle$ | $\lvert J, 5/2\ e/f\rangle$ |
|---|---|---|---|---|
| $\langle J, -1/2\ e/f\rvert$ | $T_0 - 3A/2 + 2\lambda + (z+1)(B - 3A_D/2) - D(z^2 + 5z + 1)$ | | | |
| $\langle J, 1/2\ e/f\rvert$ | $-\sqrt{3}(J+1/2)[B - A_D - 2D(z+2)] \mp \sqrt{3}(o+p+q)$ | $T_0 - A/2 - 2\lambda + (z+3)(B - A_D/2) - D(z^2 + 13z + 5) \pm (J+1/2)(p+2q)$ | symmetrical | |
| $\langle J, 3/2\ e/f\rvert$ | $-\sqrt{3(z-1)}[2D(J+1/2) \mp (1/2)(p+2q)]$ | $-2\sqrt{z-1}[B - 2D(z+2) \pm (1/4)q(J+1/2)]$ | $T_0 + A/2 - 2\lambda + (z+1)(B + A_D/2) - D(z^2 + 9z - 15)$ | |
| $\langle J, 5/2\ e/f\rvert$ | $\mp(q/2)\sqrt{(z-1)(z-4)}$ | $-2D\sqrt{3(z-1)}\sqrt{(z-4)}$ | $-\sqrt{3(z-4)}[B + A_D - 2D(z-2)]$ | $T_0 + 3A/2 + 2\lambda + (z-5)(B + 3A_D/2) - D(z^2 - 7z + 13)$ |

The centrifugal distortions of the rotation (parameter D) and the spin-orbit coupling (parameter $A_D$) were floated in the first fits, but were not determinable; they were omitted in later fits. The parameters q, p + 2q and o + p + q model the $\Lambda$-doubling.
$z = (J + ½)^2$.

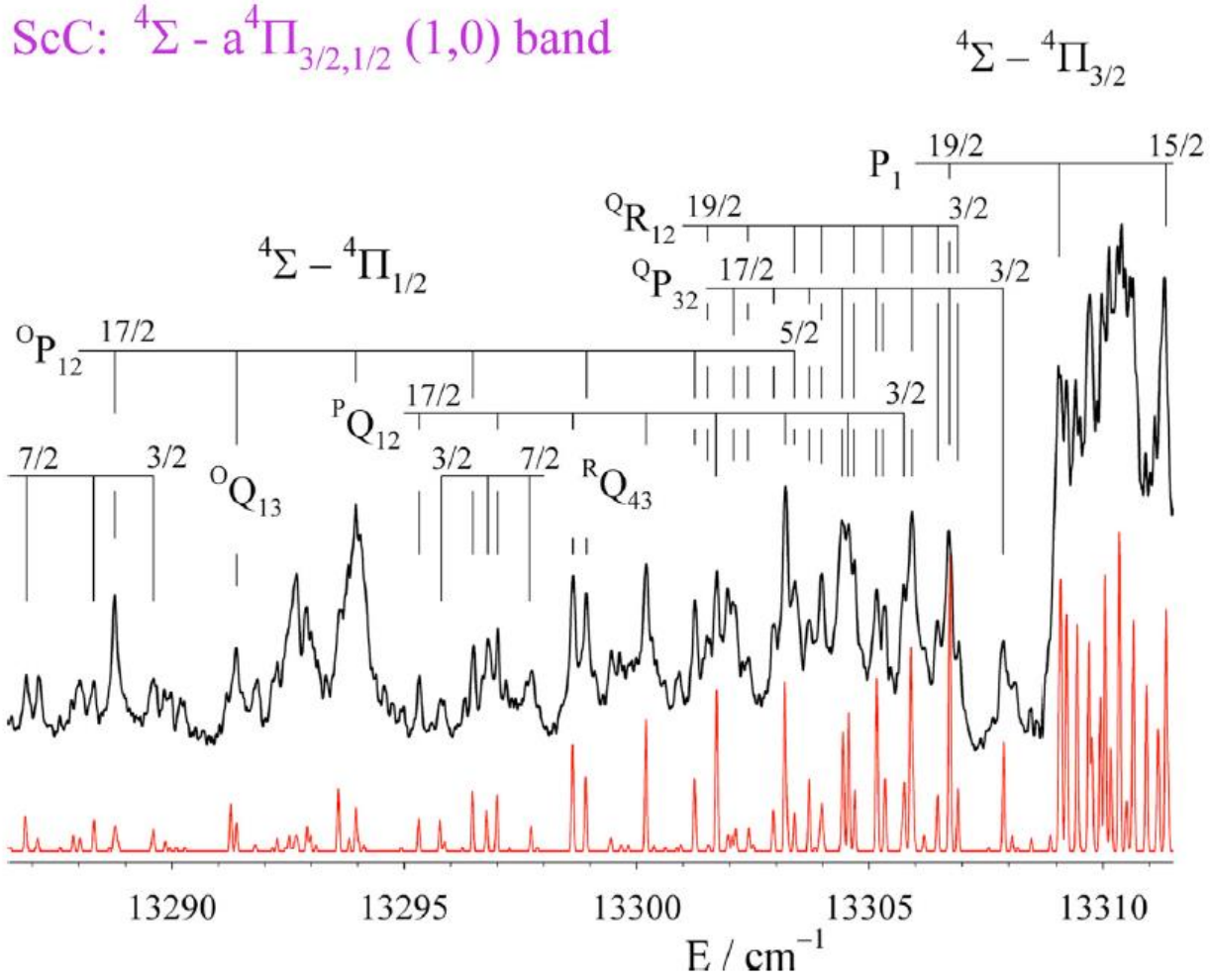


**Fig. 3.** The $Sc^{12}C$, $^4\Sigma - a^4\Pi_{3/2,\ 1/2}$, (1,0) sub-bands, with the assignments of some of the strongest branches marked. The two blue-degraded branches (assignments not marked) forming heads near 13,310 cm$^{-1}$ are $^RQ_{32}$ and $^RP_{42}$. The final band contour is also shown, with conditions as in Fig. 2.

# Prospective

1. CRD spectrum of ScC in this region to determine its oscillator strength.
2. measure the hyperfine constants and dipole moments of this band

# Laser Spectroscopy of $C_3$ Radical


1. G. Zhang, K.-S. Chen, A. J. Merer, Y.-C. Hsu, W.-J. Chen, S. Sadisavan, and Y.-A. Liao, J. Chem. Phys. **122,** 244308(2005).
2. C.-W. Chen, A. J. Merer, J.-M. Chao and Y.-C. Hsu, J. Mol. Spectrosc. **263**, 56-70(2010).
3. K.-S. Chen, G. Zhang , A. J. Merer, Y.-C. Hsu, and W.-J. Chen, J. Mol. Spectrosc. **267,** 169-171 (2011).
4. Y.-J. Wang, C.-W. Chen, L.-Z. Zhou, A. J. Merer, and Y.-C. Hsu, J. Phys. Chem. A. **117**, 13878(2013).

# Introduction

- **The spectrum of the $C_3$ , $\tilde{A}\ ^1\Pi_u - \tilde{X}\ ^1\Sigma_g^+$ system was first observed in comets by Huggins in 1882.**

- **Its first laboratory study was reported in 1942 by Herzberg and his co-workers. Since then many studies of the comet system of $C_3$ have been carried out.**
  - 1965, Gausset *et al.,* vibrational and rotational analysis of both the $\tilde{A}$ and $\tilde{X}$ states.
  - 1980, Jungen and Merer, inversion from the spectra of the $\tilde{A}$-$\tilde{X}$ system to obtain its Renner-Teller effect and Franck-Condon factors.
  - 1994, Balfour *et al*., more vibronic bands were reported.
  - 1998, Izuha and Yamanouchi, double minima found in the $\tilde{A}$ state $q_3$ coordinate.
  - 2003, McCall *et al*., reassignment of the R(0) line of the 000-000 band.
  - 2005, Zhang *et al*., perturbations of the $\tilde{A}$, 000 state have been observed and analyzed.
  - 2010, Chen *et al*., extended the study of the $\tilde{A}$ state up to 5000 $cm^{-1}$ above its zero point energy and found a strong anharmonic resonance between $\nu_1$ and $\nu_3$.

# Gerhard Herzberg

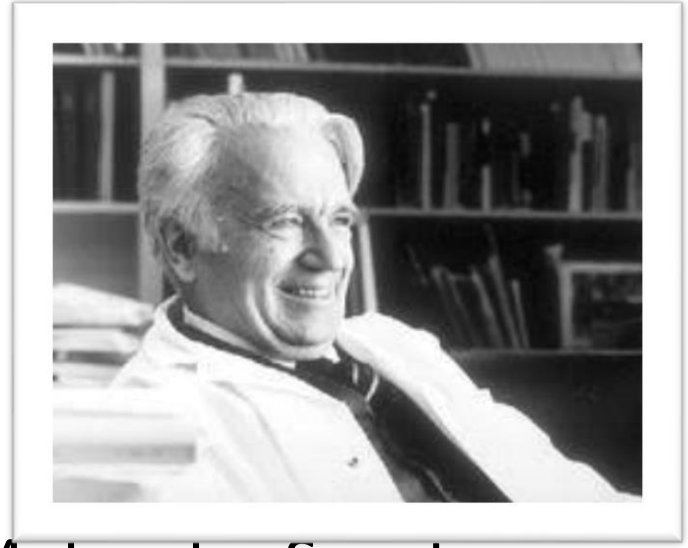

- December 1904- March 1999
- Nobel Prize in Chemistry, 1971
- Contributions to the field of Atomic and Molecular Spectrocopy
- Books:

1. Atomic Spectra and Atomic Structure, 1937
2. The spectra and structures of simple free radicals : an introduction to molecular spectroscopy.
3. Molecular Spectra and Molecular Structure – I. Spectra of Diatomic Molecules
4. Molecular Spectra and Molecular Structure –II. Infrared and Raman Spectra of Polyatomic Molecules
5. Molecular Spectra and Molecular Structure: III. Electronic Spectra and Electronic Structure of Polyatomic Molecules
6. Molecular Spectra and Molecular Structure: IV. Constants of Diatomic Molecules

# Introduction

- **The spectrum of the $C_3$ , $\tilde{A}\ ^1\Pi_u - \tilde{X}\ ^1\Sigma_g^+$ system was first observed in comets by Huggins in 1882.**

- **Its first laboratory study was reported in 1942 by Herzberg and his co-workers. Since then many studies of the comet system of $C_3$ have been carried out.**
  - 1965, Gausset *et al.,* vibrational and rotational analysis of both the $\tilde{A}$ and $\tilde{X}$ states.
  - 1980, Jungen and Merer, inversion from the spectra of the $\tilde{A}$-$\tilde{X}$ system to obtain its Renner-Teller effect and Franck-Condon factors.
  - 1994, Balfour *et al*., more vibronic bands were reported.
  - 1998, Izuha and Yamanouchi, double minima found in the $\tilde{A}$ state $q_3$ coordinate.
  - 2003, McCall *et al*., reassignment of the R(0) line of the 000-000 band.
  - 2005, Zhang *et al*., perturbations of the $\tilde{A}$, 000 state have been observed and analyzed.
  - 2010, Chen *et al*., extended the study of the $\tilde{A}$ state up to 5000 $cm^{-1}$ above its zero point energy and found a strong anharmonic resonance between $\nu_1$ and $\nu_3$.

**B. J. McCall et al, Chem. Phys. Letts 374, 583(2003)**

**(c) HD 62542**

**(b) Cavity-ring down Spectroscopy of $C_3$**

**(a) Gausset et al, Astrophys. J. 142,45(1965)**

Flash photolysis of the mixture of diazomethane and inert gas

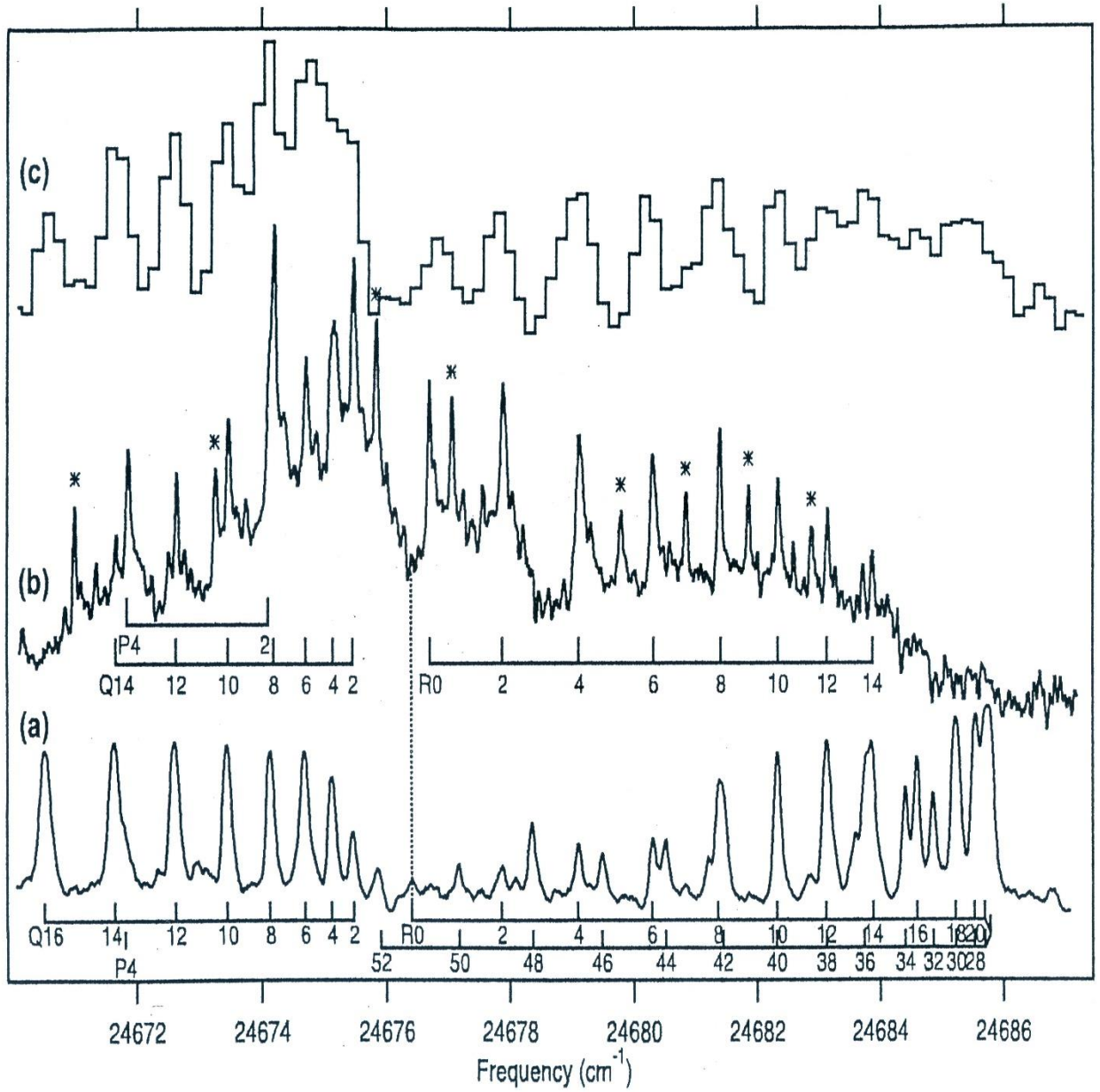

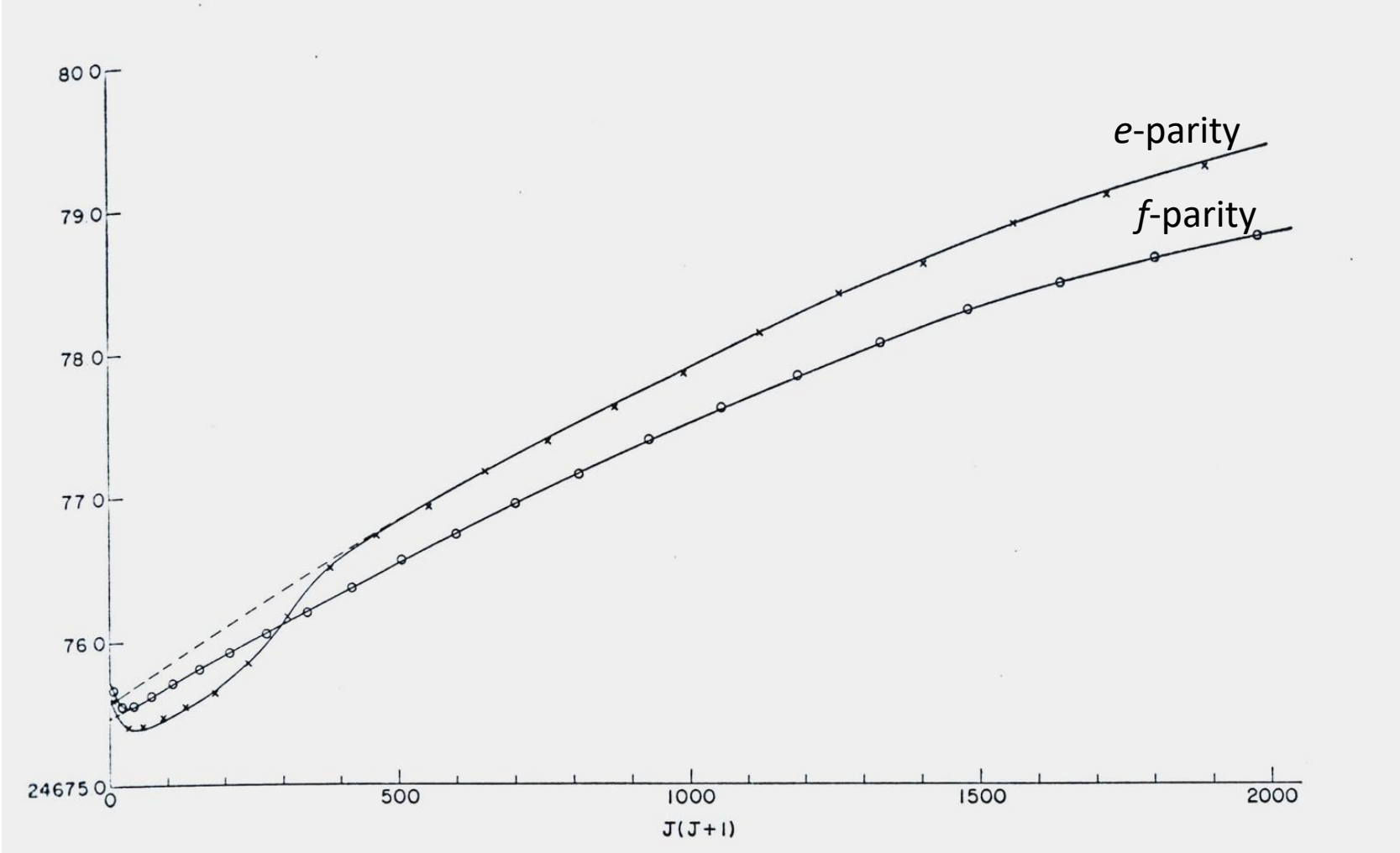


L. Gausset et. al., Astrophys. J. **42**, 45(1965)

# Fluorescence Excitation Spectra of the 000-000 band of the $\tilde{A}-\tilde{X}$ system of $C_3$

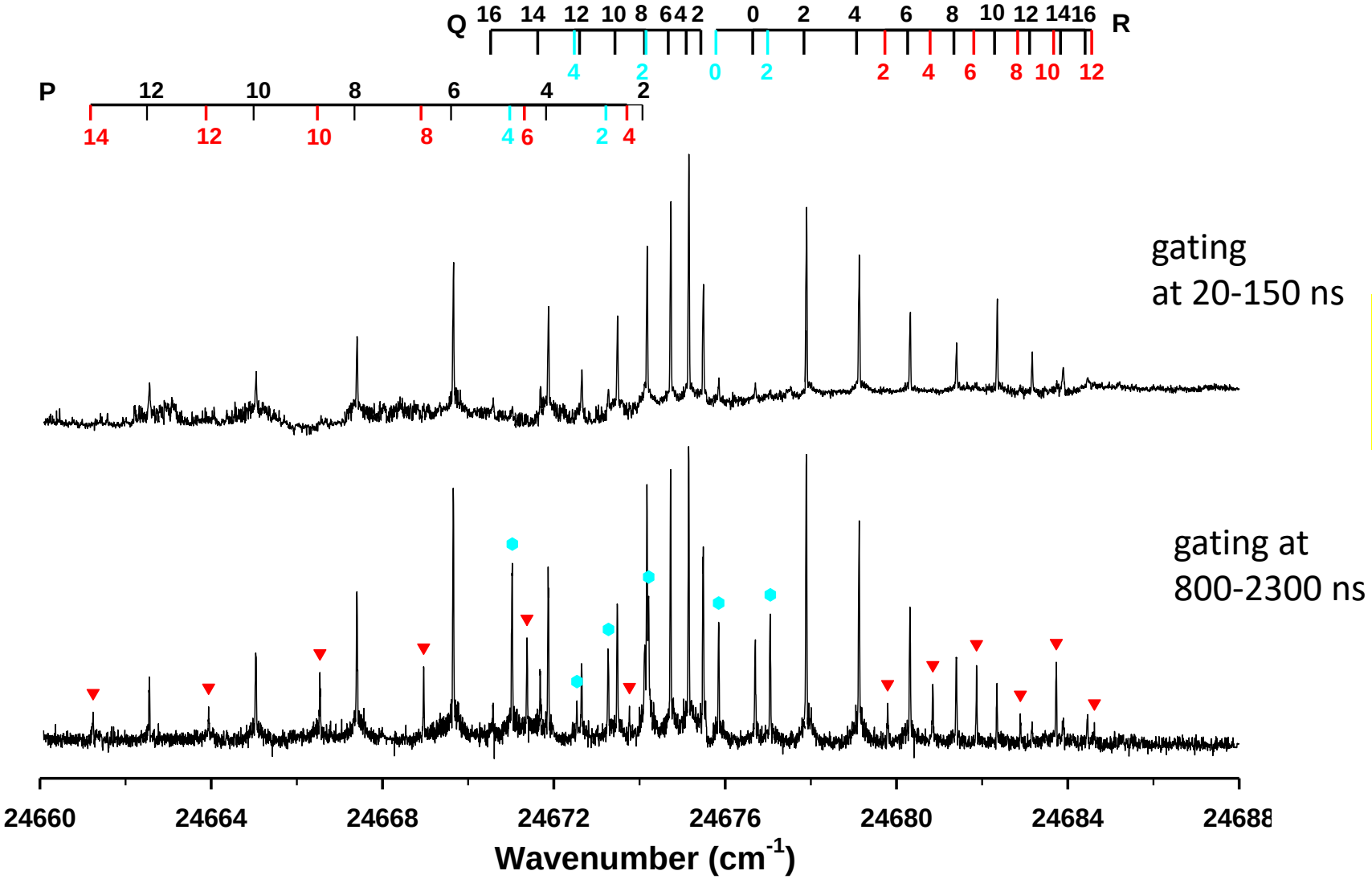


G. Zhang et. al., J. Chem. Phys. **122**, 244308(2005)

# Fluorescence Excitation Spectra of the (0,0) and $1^0_1$ bands of $C_3$

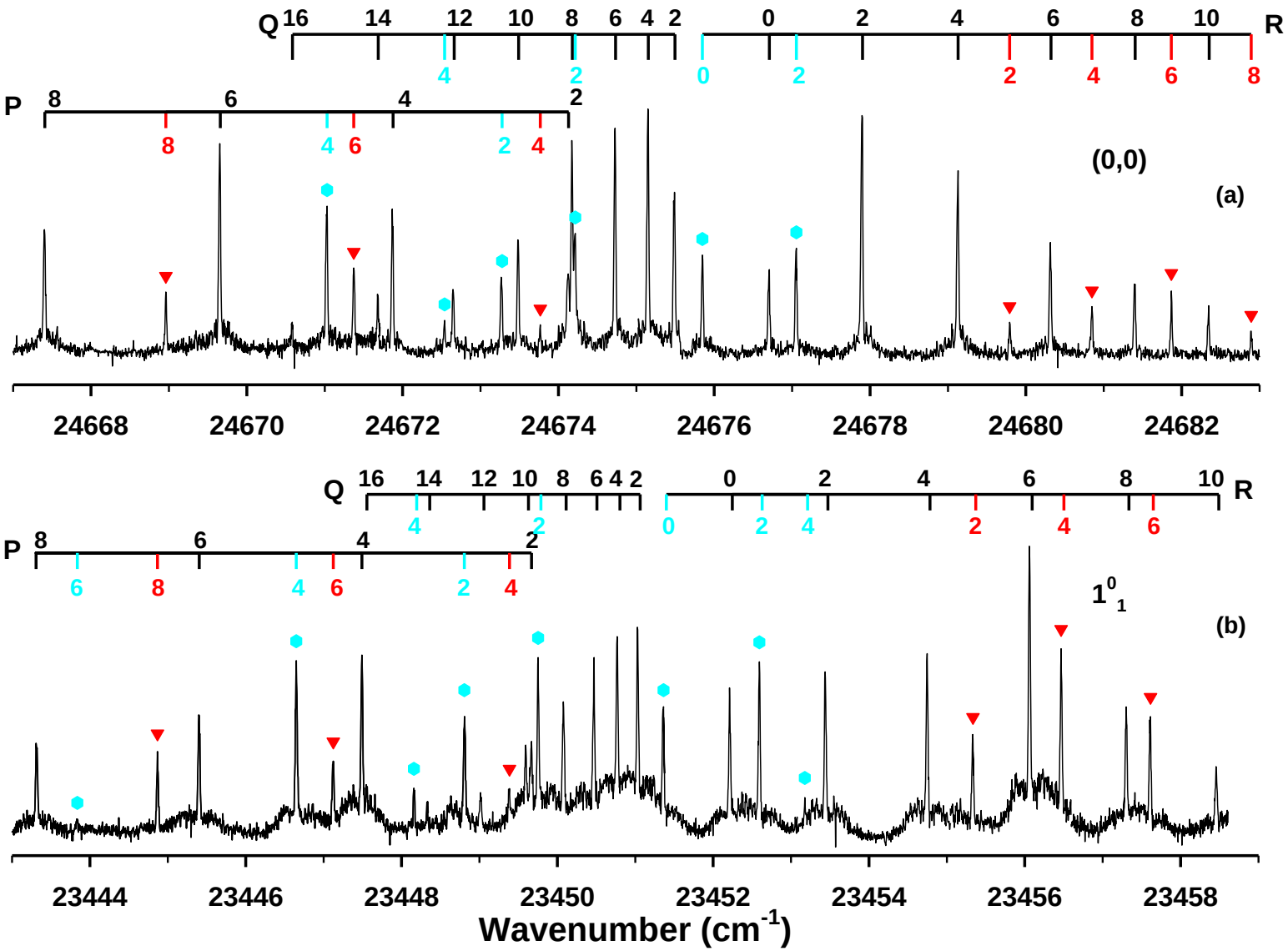


gating at
800-2300 ns

G. Zhang et. al.,
J. Chem. Phys.
**122**, 244308(2005)

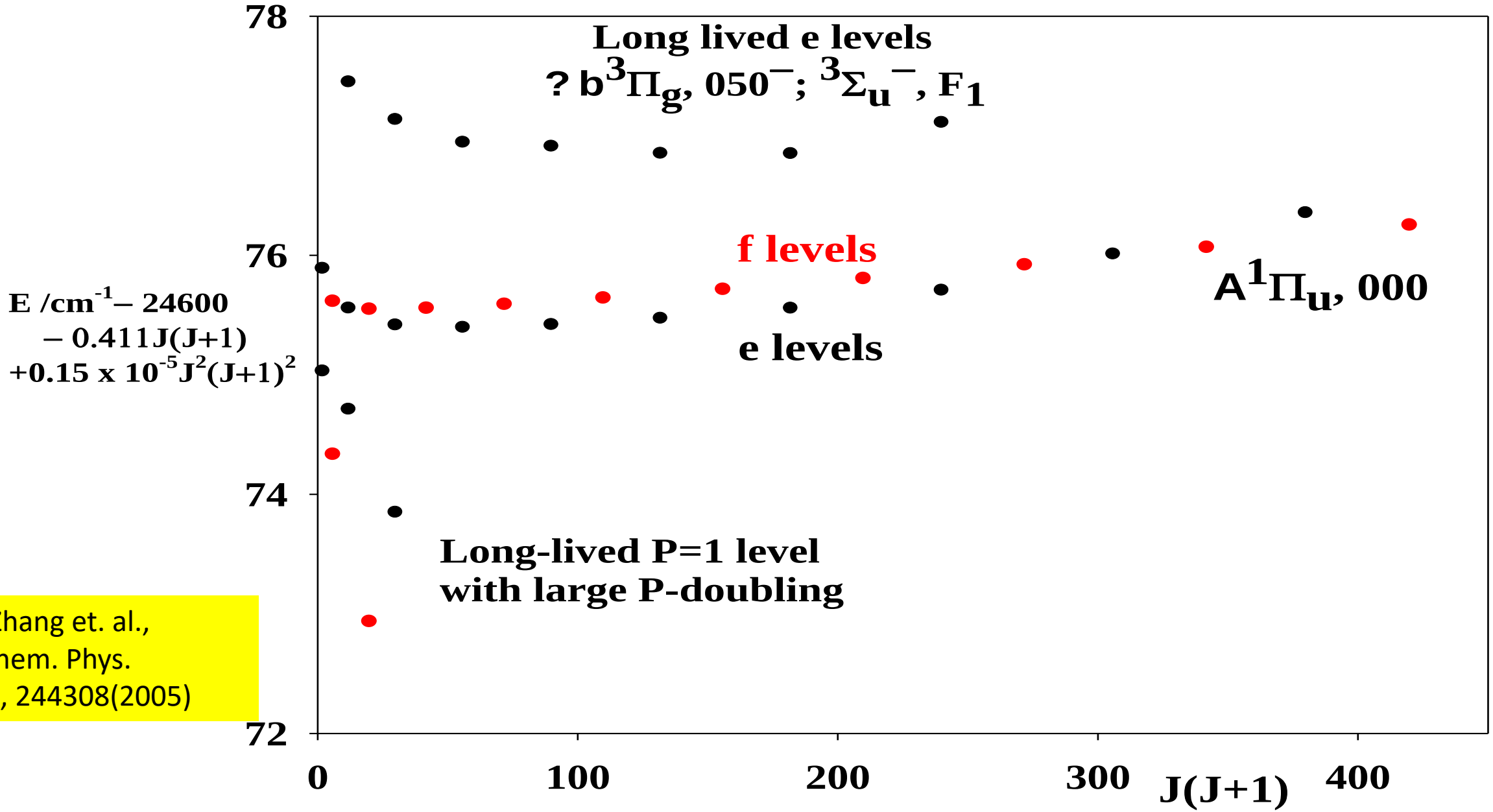


G. Zhang et. al.,
J. Chem. Phys.
**122**, 244308(2005)

**Measured lifetimes for some low-J rotational levels of the $\tilde{A}\,^1\Pi_u$, 000 state of $C_3$ (Values in parentheses represent three standard deviation of the fit.)**

**Single exponential decays (Main band)**

| Line | Wavenumber/cm$^{-1}$ | $\tau$/ns |
|---|---|---|
| R(2) | 24677.907 | 227(6) |
| R(4) | 24679.134 | 214(15) |
| R(6) | 24680.329 | 212(2) |
| Q(2) | 24675.498 | 209(6) |
| Q(4) | 24675.158 | 195(9) |
| Q(6) | 24674.736 | 192(6) |
| P(4) | 24671.878 | 227(6) |

**Bi-exponential decays (Perturbing states)**

| Line | Wavenumber/cm$^{-1}$ | $\tau_1$/ns | $\tau_2$/ns |
|---|---|---|---|
| P(2) | 24673.270 | 237(4) | 470(15) |
| P(4) | 24671.032 | 786(5) | 202(5) |
| R(2) | 24677.058 | 752(51) | 216(26) |
| R(2) | 24679.798 | 223(10) | 2190(600) |

G. Zhang et. al., J. Chem. Phys. **122**, 244308(2005)

**Rotational constants derived by least squares from our data for the $\tilde{A}\ ^1\Pi_u$, 000 state of $C_3$ and its perturbing states. Values in $cm^{-1}$.**

| | | | | | |
|---|---|---|---|---|---|
| $T_0^{\Pi}$ | 24675.632 ± | 0.080 | $T_0^{\Sigma}$ | 24682.12 ± | 0.74 |
| $B^{\Pi}$ | 0.41261 | 0.00030 | $B^{\Sigma}$ | 0.4411 | 0.0032 |
| $10^6\ D^{\Pi}$ | 0.298 (fixed) | | $\lambda$ | –7.22 | 1.32 |
| $q^{\Pi}$ | –0.00125 | 0.00059 | $T_0^{P}$ | 24675.68 | 0.14 |
| $\xi$ | 0.744 | 0.063 | $B^{P}$ | 0.3154 | 0.0072 |
| $a$ | 0.436 | 0.060 | $q^{P}$ | –0.076 | 0.007 |

r.m.s. error 0.0366

G. Zhang et. al.,
J. Chem. Phys. **122**, 244308(2005)

Schmidt et. al, MNRAS **441**, 1131(2014)

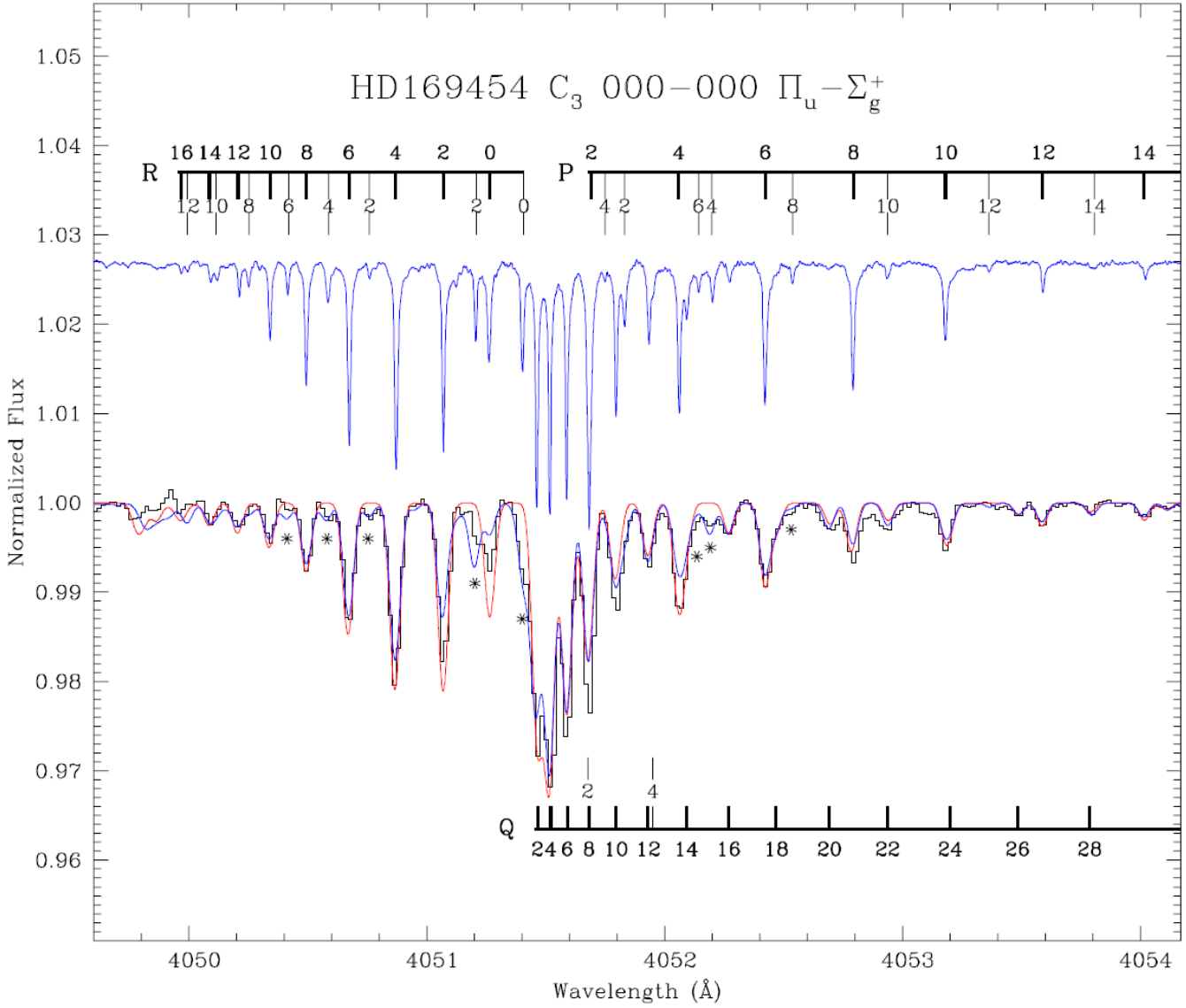


**Figure 2.** Spectrum of the $C_3$ $\tilde{A}^1\Pi_u$ - $\tilde{X}^1\Sigma_g^+$ 000–000 band. Upper spectrum: laboratory measurement by cavity ring-down spectroscopy in a planar plasma jet. Lower spectrum: observation in the sightline to HD 169454. Positions of rotational lines are tagged with thick lines. Thin lines tag rotational lines due to perturbing states based on the analysis of Zhang et al. (2005). The astronomical spectrum is overlaid with fitted curves: the red curve represents a fit using only unperturbed lines; for the blue curve perturber lines are included in the fit. Note the remaining deviation for the intensity of the R(0) line in the simulated spectrum (see text).

Schmidt et. al, MNRAS **441**, 1131(2014)

**Table 7.** Summary of observed molecular column densities towards HD 169454.

| Molecule | $N_{col}$ ($10^{12}$ cm$^{-2}$) | $T_{exc}$ (K) | Source |
|---|---|---|---|
| $C_2$ | $65 \pm 1$ | $19 \pm 2$ | 1 |
| | $73 \pm 14$ | $15^{+10}_{-5}$ | 2 |
| | $70 \pm 14$ | | 3 |
| | $160 \pm 29$ | | 4 |
| $C_3$ | $6.61 \pm 0.19$ | $22.4 \pm 1.0$ | 5 |
| | $2.24 \pm 0.66^a$ | $23.4 \pm 1.4$ | 4 |
| | $4.5 \pm 0.3^b$ | | 3 |
| CH | $39.6 \pm 0.3^c$ | | 5 |
| | $46 \pm 8$ | | 2 |
| | $36.5^{+12.6}_{-7.8}$ | | 6 |
| $CH^+$ | $20.8 \pm 0.2^e$ | | 5 |
| $H_2$ | $(8 \times 10^{20d})$ | | 5 |

[a]Based on a sample of rotational lines with $J \leq 8$.
[b]Based on unresolved rotational lines.
[c]Based on CH line at 3886.409 Å.
[d]Based on correlation of CH w.r.t. $H_2$ (Weselak et al. (2004); fig. 3. therein).
[e]Based on the $CH^+$ line at 3957 Å.
Source: (1) Kazmierczak et al. (2010a); (2) Jannuzi et al. (1988); (3) Oka et al. (2003); (4) Ádámkovics et al. (2003); (5) This work; (6) Crawford (1997).

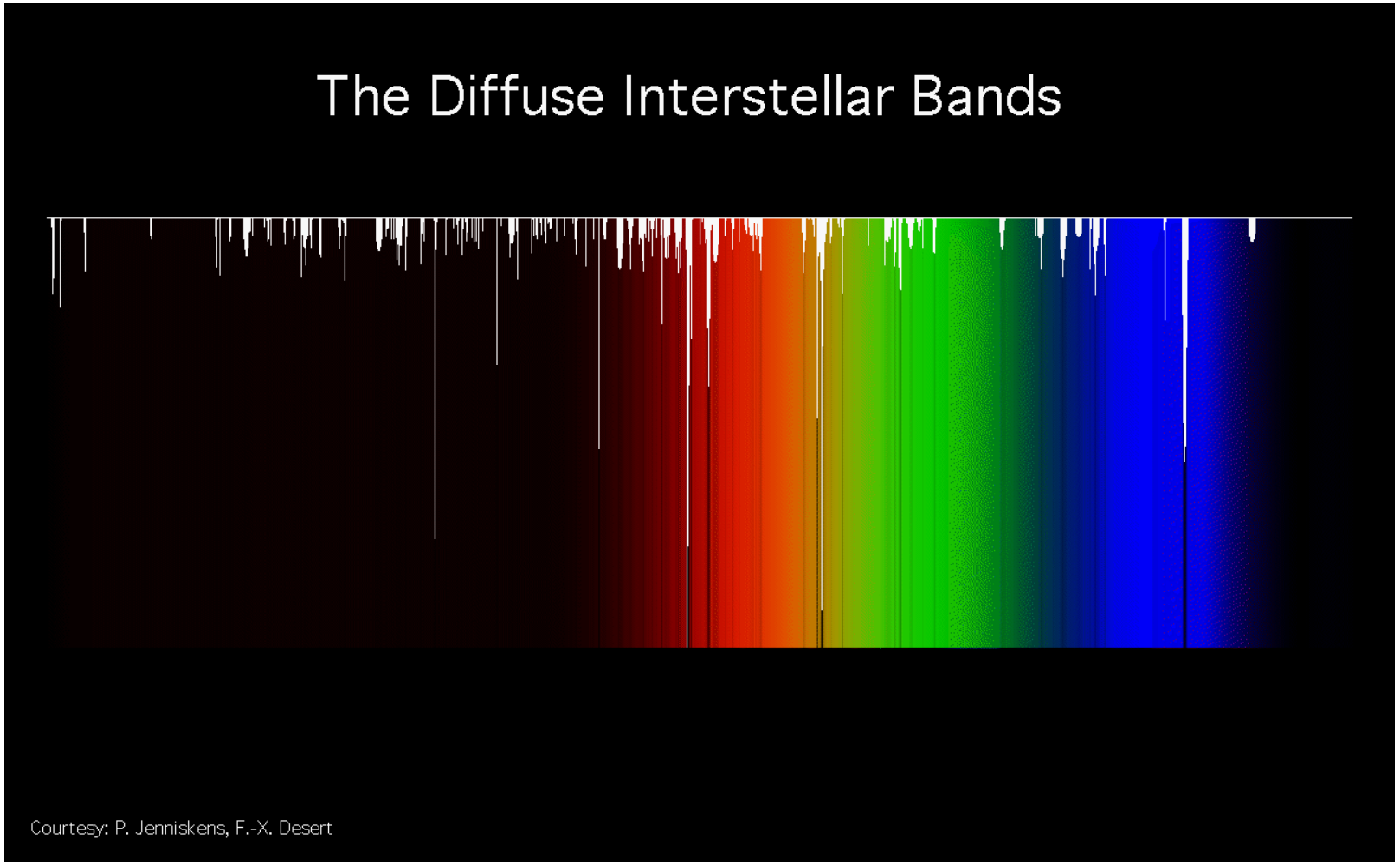


Absorption features seen in the spectra of astronomical objects in the Milky Way and other galaxies.
They are caused by the absorption of light by the intersetller medium. About 500 bands have now been seen, in UV, visible, and IR.

The origin of DIBs was unknown and disputed for many years, and the DIBs were long believed to be due to polycyclic aromatic hydrocarbons and other large carbon-bearing molecules.

Schmidt et. al, MNRAS **441**, 1131(2014)

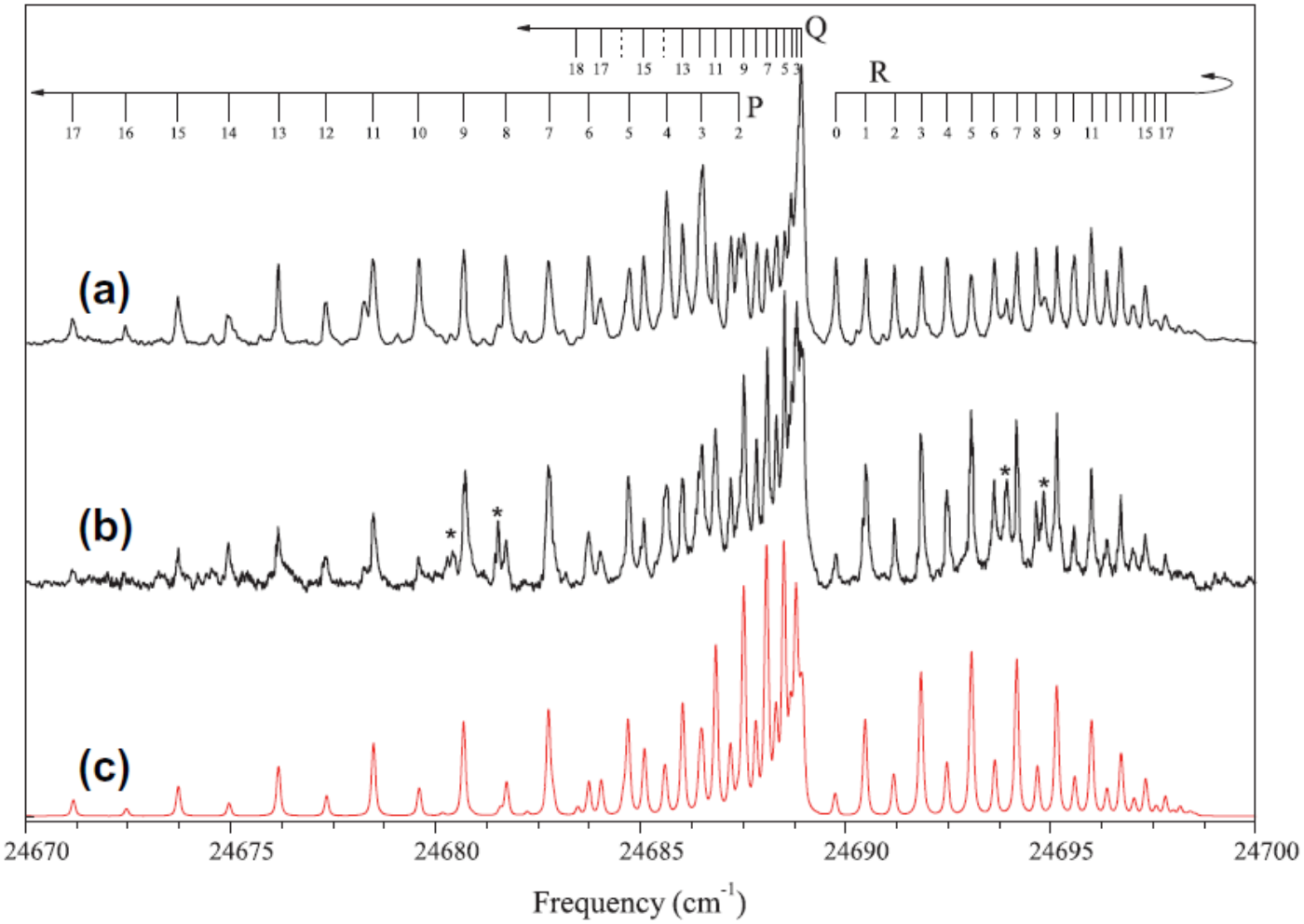


**Fig. 2.** Rotationally resolved spectra of the $\tilde{A}^1\Pi_u - \tilde{X}^1\Sigma_g^+$ electronic origin band of $^{13}C_3$. (a) Saturated spectrum recorded with ~0.2% of $^{13}C_2H_2$ in the gas mixture; (b) Spectrum recorded with ~0.03% of $^{13}C_2H_2$ in the gas mixture yielding reliable intensities. (c) The red trace shows the simulated spectrum for a $^1\Pi_u - ^1\Sigma_g^+$ transition, with derived constants for $^{13}C_3$, a Lorentzian width of 0.07 $cm^{-1}$, a Gaussian width of ~0.1 $cm^{-1}$, and an estimated rotational temperature of ~45 K. The lines marked with an asterisk are due to blending transitions of other small species like $^{13}C_2$ or $^{13}CH$, etc. (For interpretation of the references to color in this figure legend, the reader is referred to the web version of this article.)

No perturbation was observed in their $^{13}C_3$, 000-000 band (lab), consistent with our assignments. Perhaps next generation telescope would allow us to observe the transition of $^{13}C_3$.

# Laser spectroscopic studies of $C_3Ar$ van der Waals complex


1. G. Zhang, B.-G. Lin, S.-M. Wen, and Y.-C. Hsu, J. Chem. Phys. **120**, 3189-3200(2004).

2. A. J. Merer, Y.-C. Hsu, Y.-R. Chen, and Y.-J. Wang, J. Chem. Phys. **143**, 194304(2015).

3. Y.-J. Wang and Y.-C. Hsu, (to be published).

# The Normal Modes of $C_3$-Rg Complex

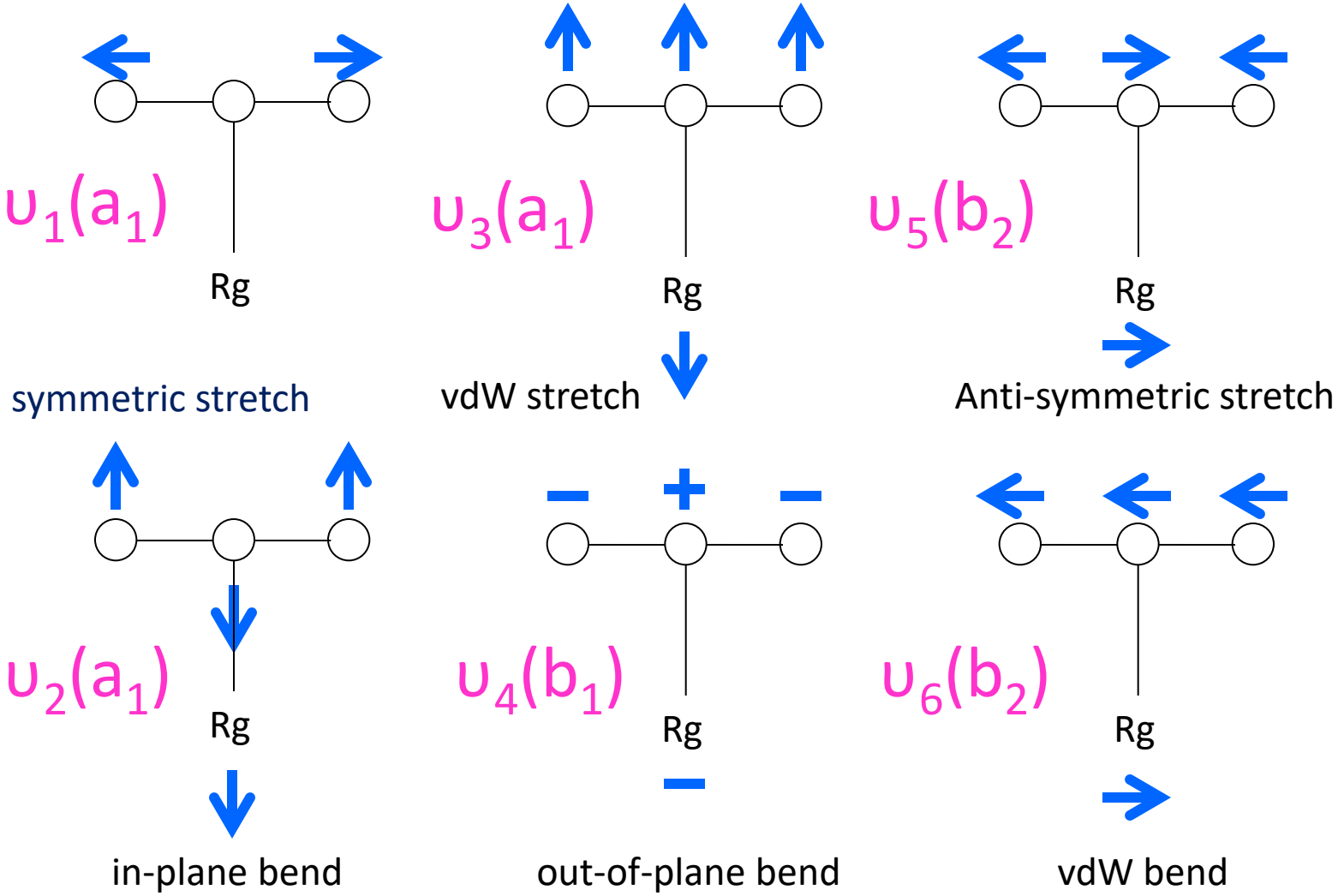

# Unique feature of $C_3(\tilde{X})$

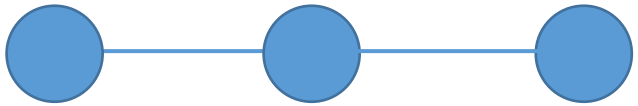

$\tilde{X}^1\Sigma_g^+$

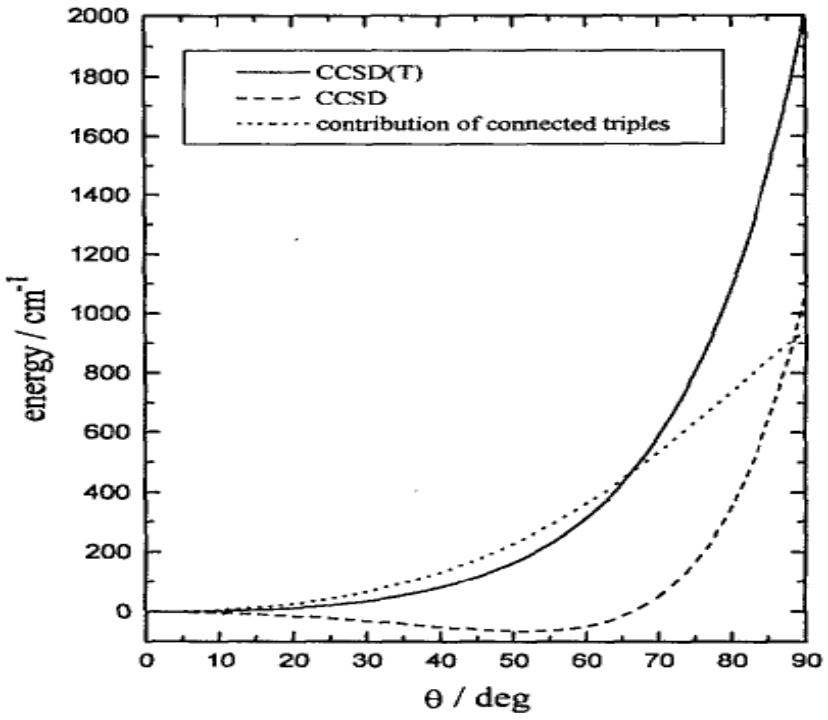


Unusually low bending frequency
63 $cm^{-1}$
Schmuttenmaer et. al., Science (1990)

Mladenović et.al., J. Chem. Phys. **101**, 5891 (1994).

How would the rare gas atom affect the large amplitude motion of $C_3$?

# Unique features of $C_3(\tilde{A})$

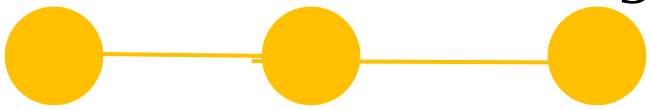

$\tilde{A}\ ^1\Pi_u$

**Non-equivalent C-C bond lengths** was observed in the $\tilde{A}$ state.

**Large Renner Effect** was reported in the $\tilde{A}$ state (Gausset et. al., Astrophys. J. 1965)
Due to the static effect set up by molecular bending motion and $\pi$- orbital, the degeneracy of the $\Pi$ state is lifted.------ **A failure of B-O approxiamation**.

**$K=\Lambda+\ell$ , *good*** quantum number

**K**: projection of total angular momentum onto the principle axis of $C_3$

**$\Lambda$:** projection of electronic angular momentum onto the principle axis of $C_3$

**$\ell$ :** vibrational angular momentum

# The **Renner-Teller Effect** of the $\tilde{A}$ state of $C_3$

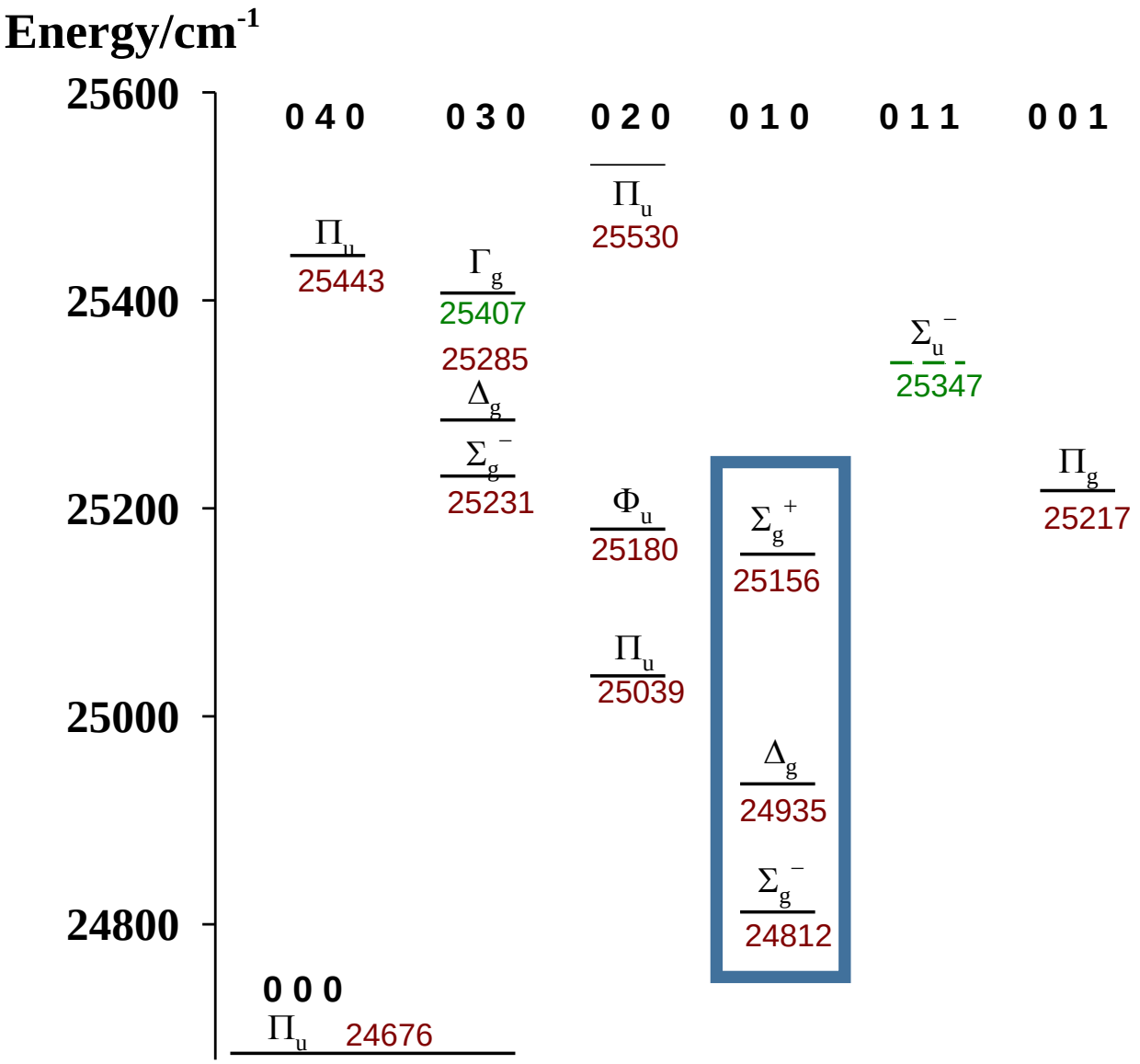


**K=Λ+ ℓ** , ***good*** quantum number

**K**: projection of total angular momentum onto the principle axis of $C_3$

**Λ:** projection of electronic angular momentum onto the principle axis of $C_3$

**ℓ :** vibrational angular momentum

Chen et. al., J. Mol. Spectrosc. **267,** 169-171 (2011).

# LIF Excitation Spectra of $C_3Ar$ and $C_3$

- ***In the region 25410-25535 cm$^{-1}$***

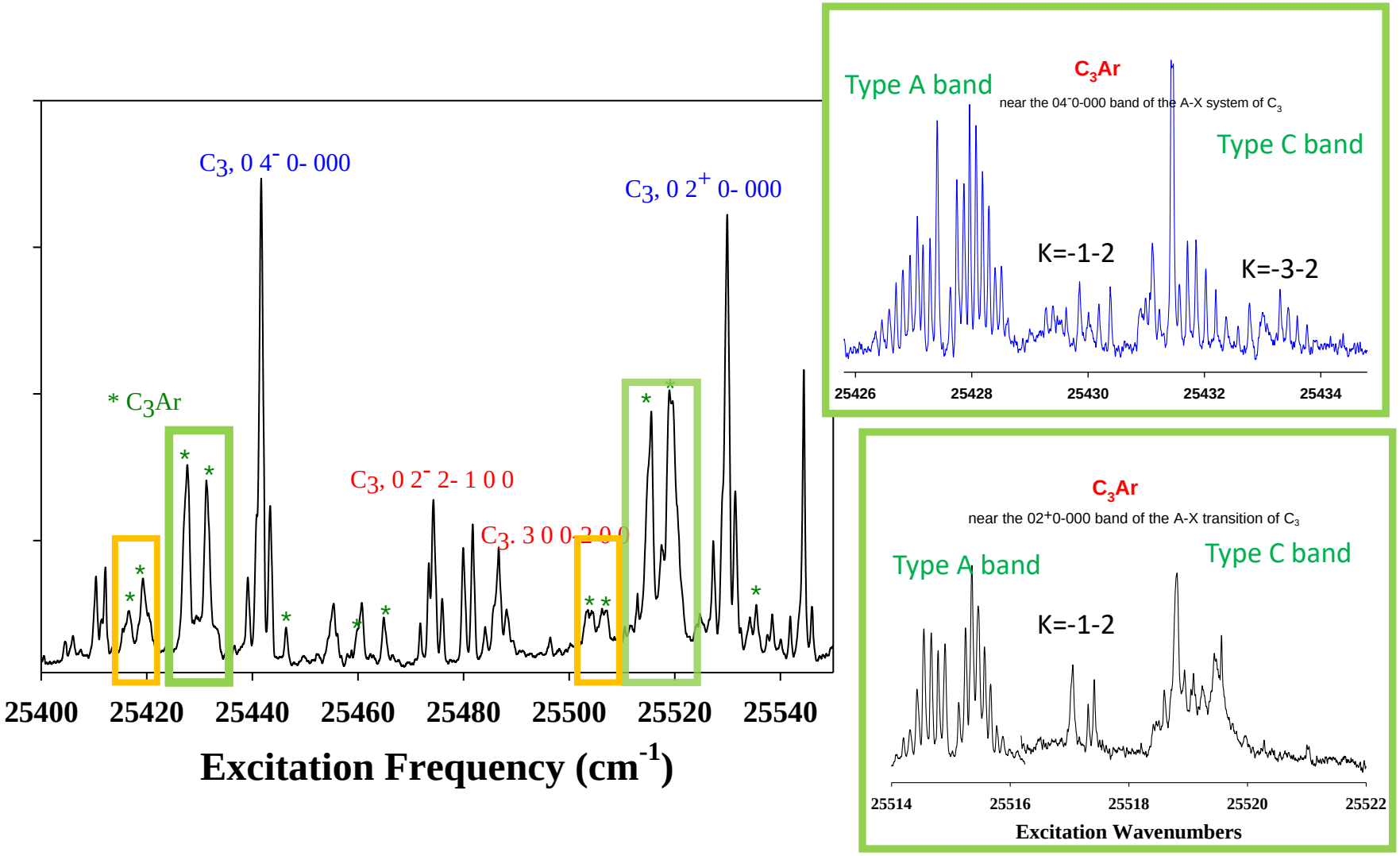

# Band Contour Analysis of Type C band

$C_3Ar$: $04\bar{1}0$ Type C band

Observed spectrum

Calculated with T = 1.7 K;
and FWHM = 0.035 $cm^{-1}$

$$\Delta K_a, \Delta K_b = \pm 1, \Delta K_c = 0$$

| | 3σ |
|---|---|
| $T_0$ = 25434.881 | (3) |
| A = 0.4429 | (10) upper |
| B = 0.066069 | (324) |
| C = 0.054388 | (769) |
| $\Delta_K$ = −0.000067 | (40) |
| A = 0.4551 | (10) lower |
| B = 0.059934 | (1199) |
| C = 0.054375 | (1200) |
| rms = 0.0025 | |

$\Delta'' = -8.3$ amu $Å^2$

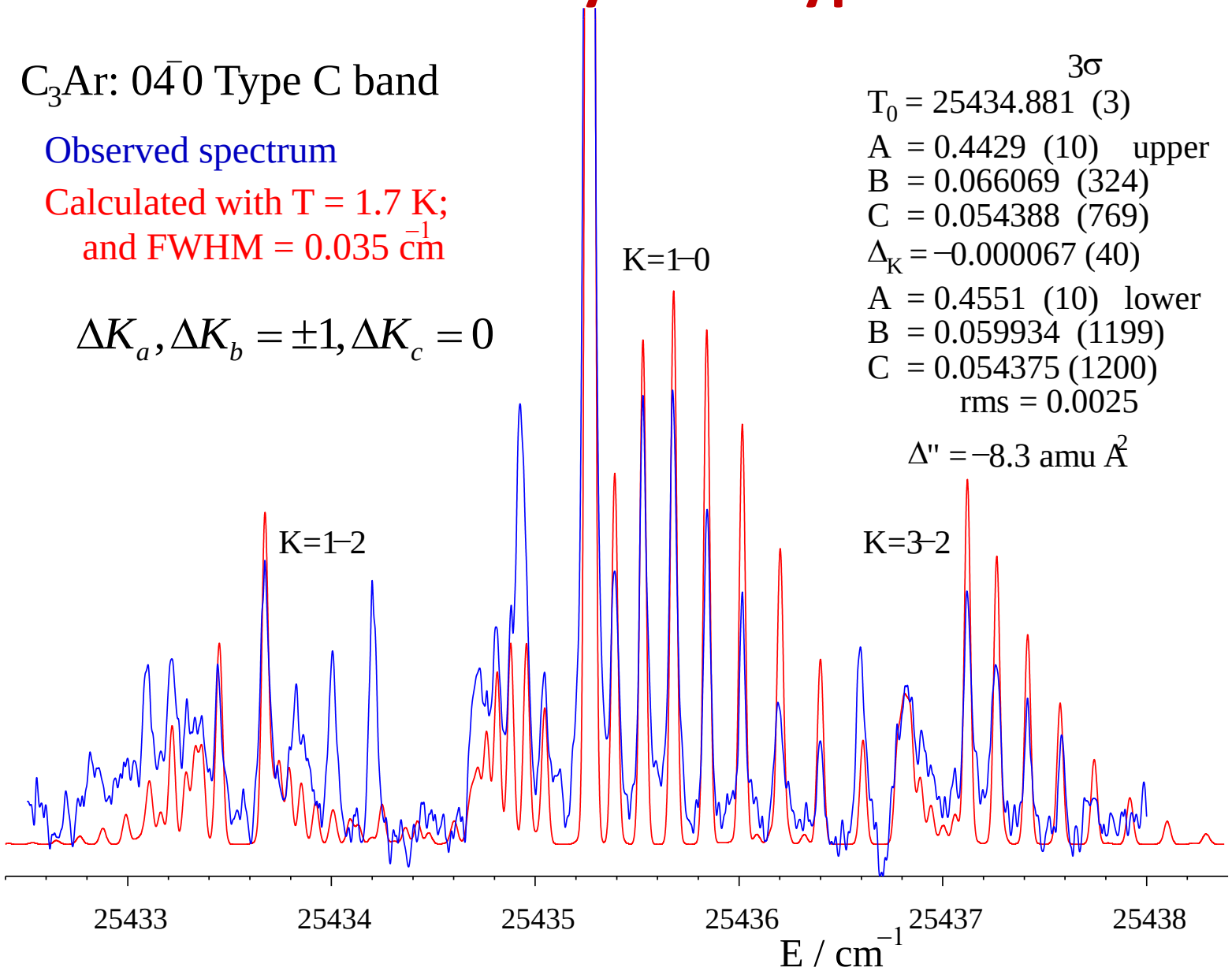

# Band Contour Analysis of Type A band

$C_3Ar$: $04^{-}0$ Type A band

Observed spectrum

Calculated, with T = 1.7 K
and FWHM = 0.035 $cm^{-1}$

3σ

$T_0$ = 25431.334 (4)
A' = 0.4284 (16)
B' = 0.059156 (2330)
C' = 0.054934 (1805)
A" = 0.4551 (*f*)
B" = 0.059934 (*f*)
C" = 0.054956 (291)
rms = 0.0025

Δ" = –11.57 amu $A^2$

$\Delta K_a = 0, \Delta K_b, \Delta K_c = \pm 1$

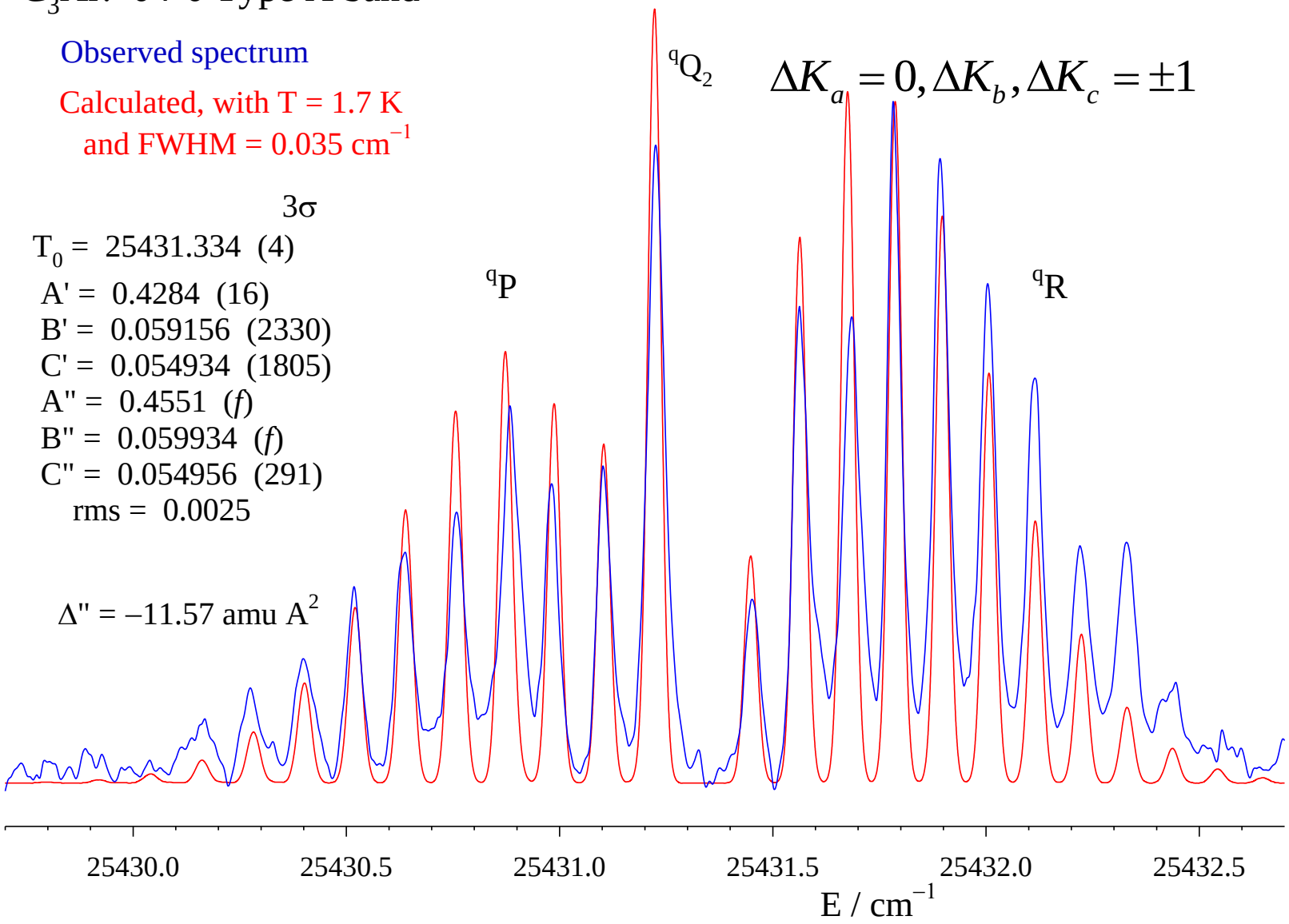

# Summary of the ROTATIONAL information of the v=0 of $C_3Ar(\tilde{X})$

1. K″=0 and 2 levels were observed in the LIF spectra.
   The $^{12}C$ nucleus is a boson, therefore the Ar atom must lie in the $C_{2v}$ axis of $C_3Ar$, T-shaped.
2. From rotational analysis, the rotational constant A is greater than the rotational constant B of $C_3$.
   Experimentally obtained rotational constants are consistent with those calculated from the predicted wavefuntions by MCTDH within 95%.
   The rotational constants B and C give the vdW bond length as 3.81Å .
3. The electronic degeneracy ($^1\Pi_u$) of the upper state is lifted in the lower symmetry of the complex. Each $\Pi_u$ vibronic upper level splits into an $A_1$ and $B_1$ pair.

Merer et. al., J. Chem. Phys. **143**, 194304 (2015).

# The **geometry** and **probability** of the v=0 of $C_3Ar(\widetilde{X})$ **from the MCDTH calculation using an ab initio potential at the level of CCSD(T)/pVQZ**

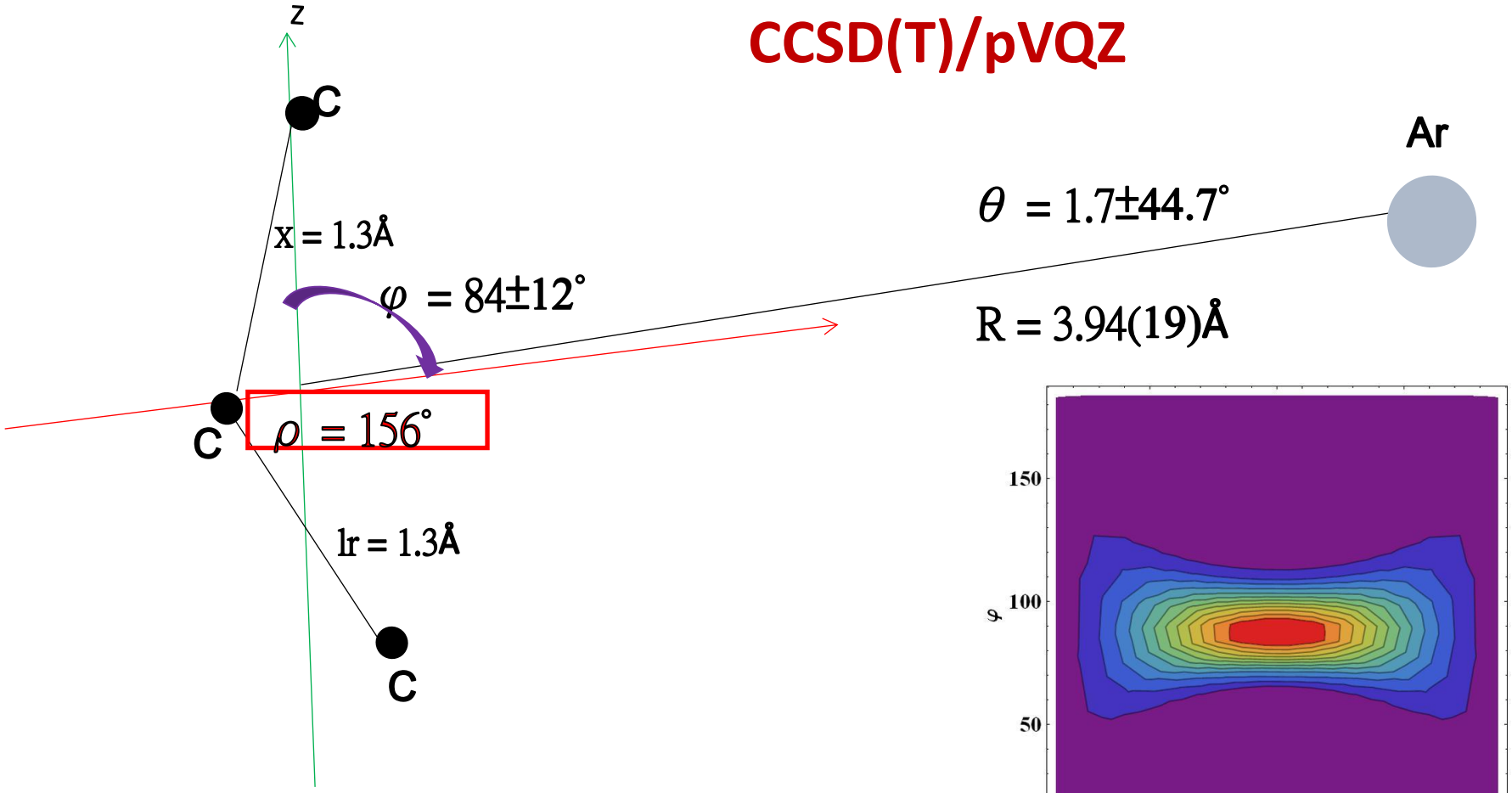


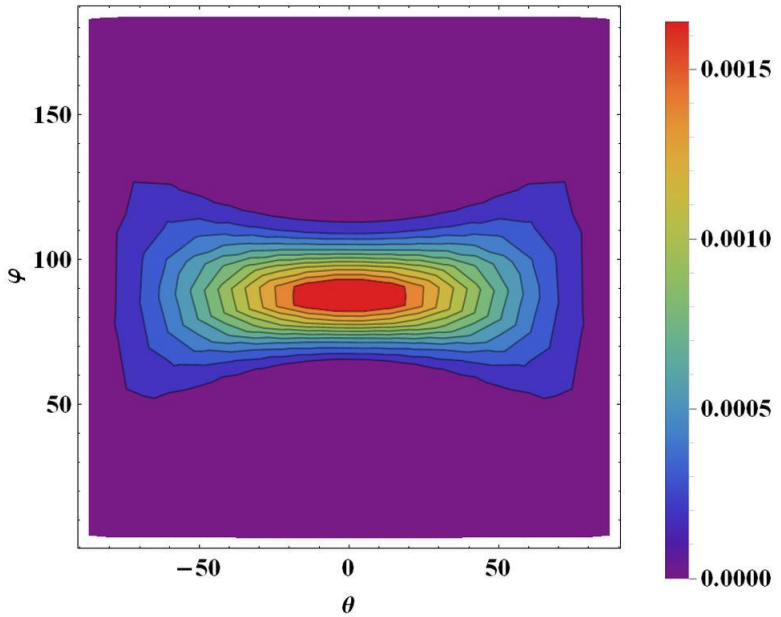


**The contour plot of probability distribution was obtained at**

**R 3.814Å , $r_1$=1.3002Å , $r_2$=1.3071Å , ∠C-C- C=156.9°**

# •*Predissociation pathways of $C_3Ar$ near the 25039 $cm^{-1}$ region*

$$C_3Ar(\tilde{A}^1\Pi_u) \xrightarrow{\text{predissociate}} C_3\ \text{fragments}\ (\tilde{A}^1\Pi_u) + Ar$$

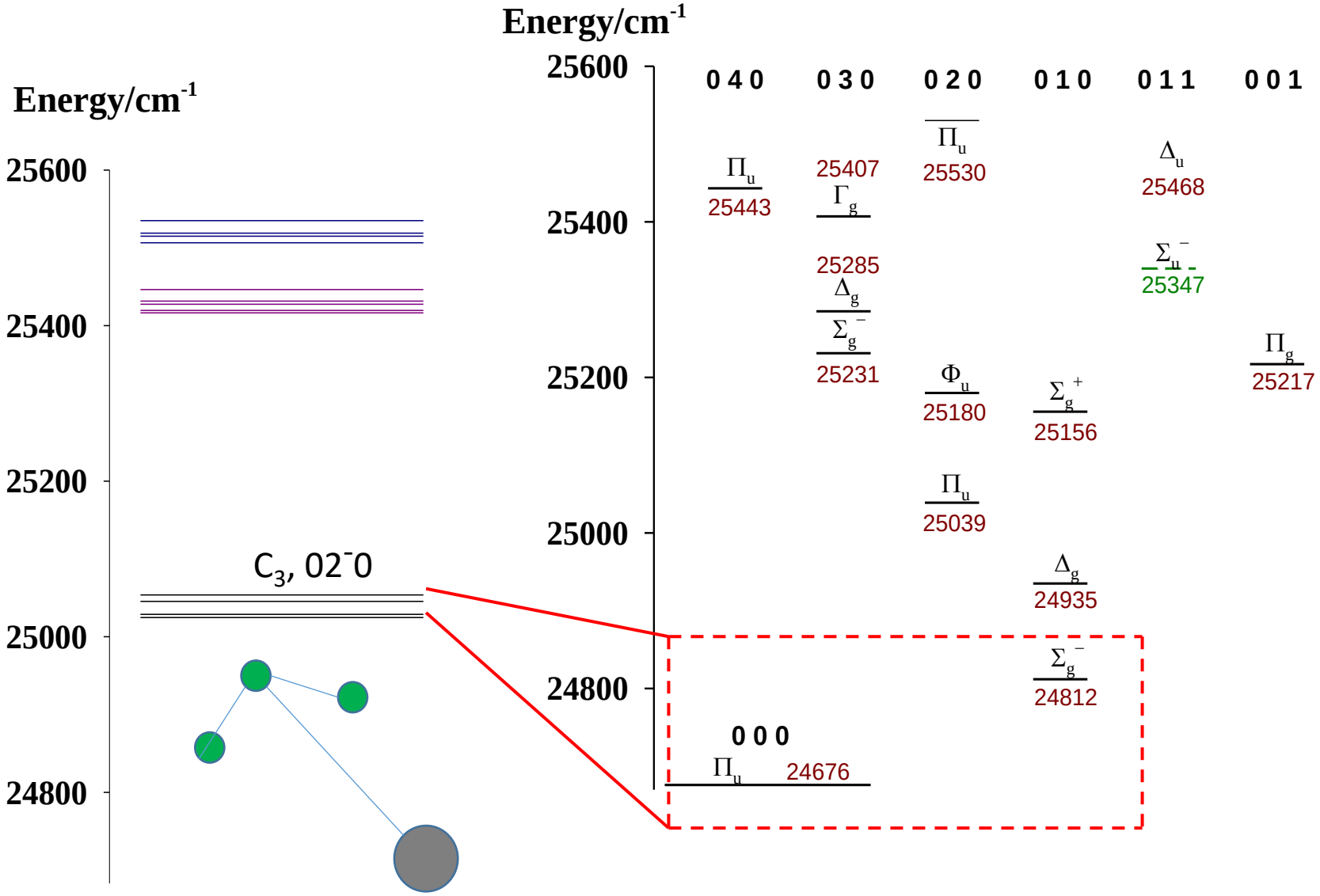

# •*Predissociation pathways of $C_3Ar$ near the 25416-25520 $cm^{-1}$ region*

$$C_3Ar(\tilde{A}^1\Pi_u) \xrightarrow{\text{predissociate}} C_3\ \text{fragments}\ (\tilde{A}^1\Pi_u) + Ar$$

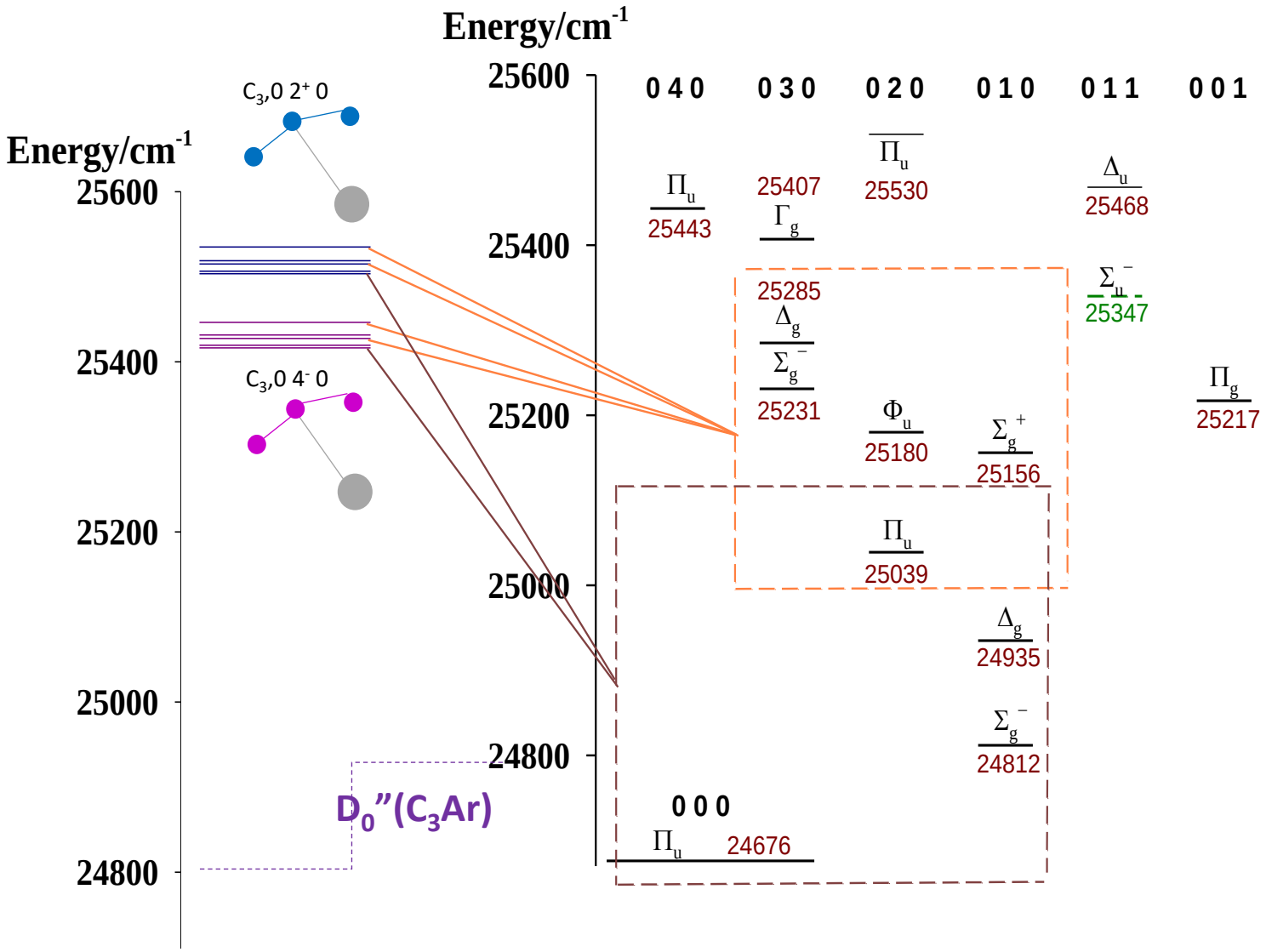

# **Relaxation** observed in the emission spectra of $C_3Ar$ from the **25431 cm$^{-1}$** band

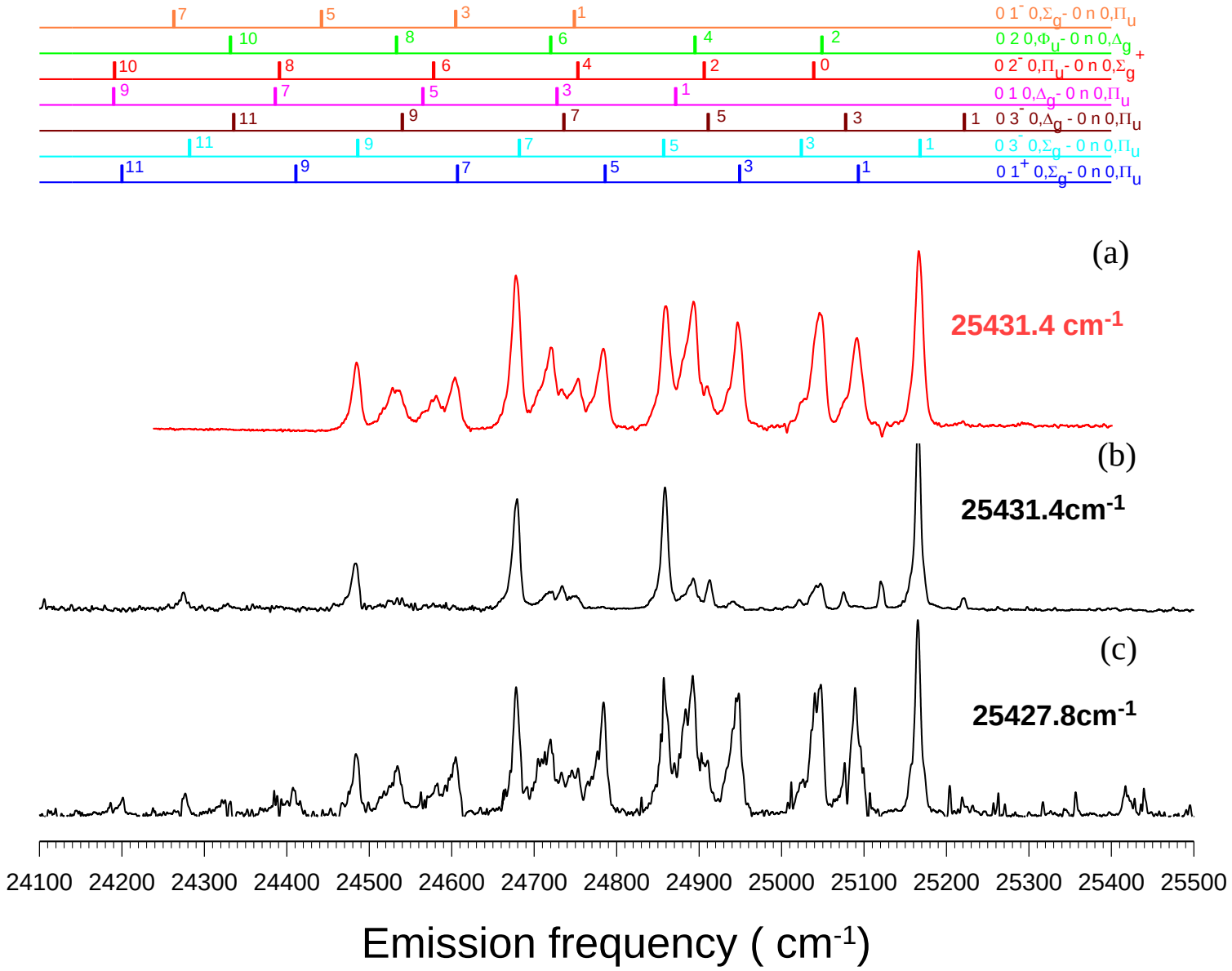


(a): separation of pump-probe lasers is ~20mm
(b) and (c);
separation of pump-probe lasers is ~36 mm

The 25431 cm$^{-1}$ band of $C_3Ar$ can be a suitable system to generate an unique source of odd-$v_2$ level of $C_3$.

From the bluest feature of the 25427.8 cm$^{-1}$ band, the upper bound of D0" of $C_3Ar(\tilde{X})$ can be determined as 143 cm$^{-1}$, consistent with our ab initio calculation.

# $C_3Ar$ relaxation observed from the 26689 $cm^{-1}$ level near the $C_3$, $02^{-}2$-100 band

- E(A, 012) =26476 $cm^{-1}$.
- Although $09^{-}0$ and $01^{-}2$ levels are nearly degenerate. Only $\Delta v_2$=1-2 transfer are prominently seen.

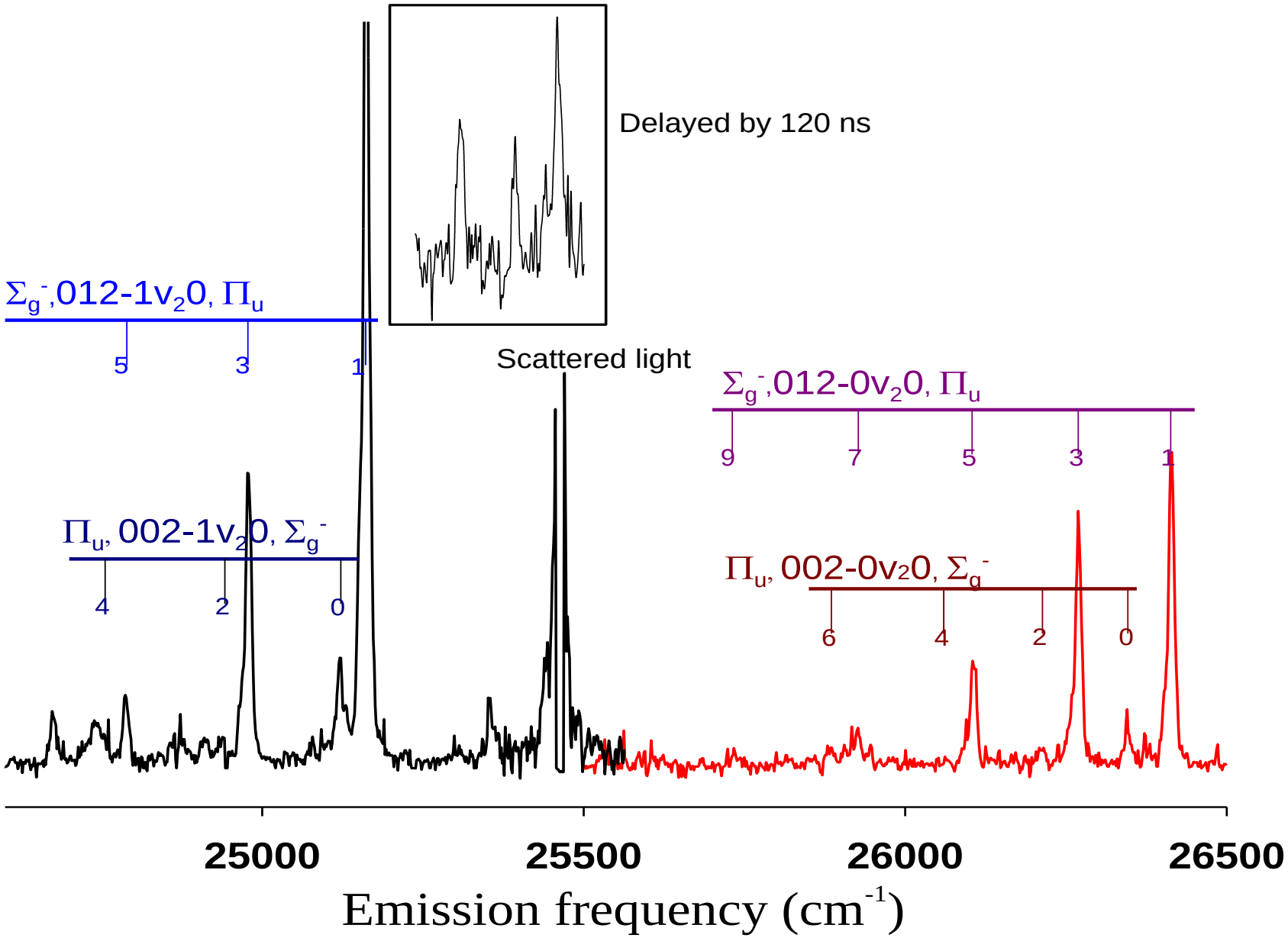

# Estimated energy disposals of the predissociation products

| **Green** bands | | **Orange** bands | |
|---|---|---|---|
| R | 30 $cm^{-1}$ | | |
| T | ~120 $cm^{-1}$ | R+T | ~420 $cm^{-1}$ |
| V | ~540 $cm^{-1}$ | V | ~260 $cm^{-1}$ |

# Hole burning experiment

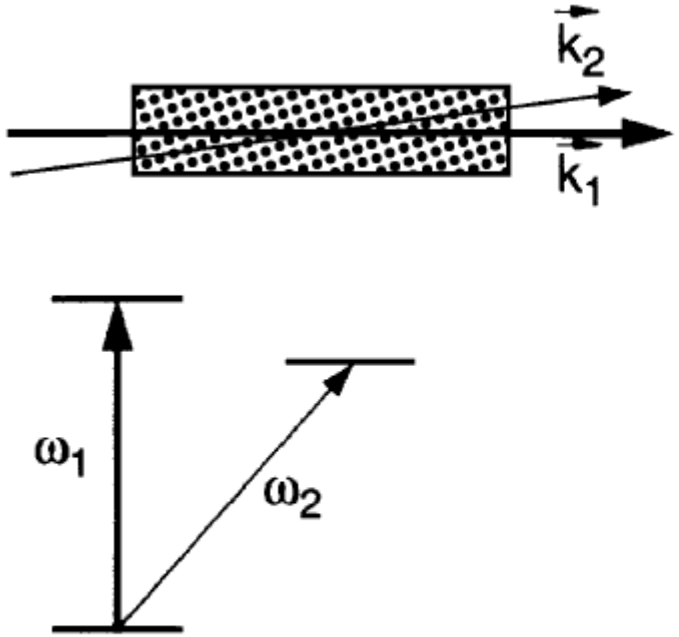


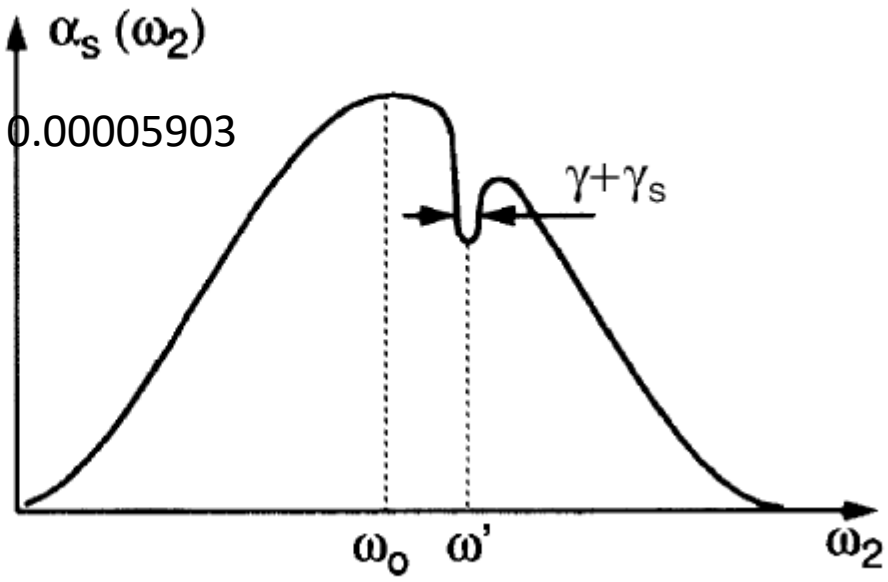


$$\omega' = \omega_o + (\omega_1 - \omega_o)\, k_1 / k_2$$

# UV-UV Hole burning experiment of the *rotationally resolvable* bands

Scanning the type C band of $\tilde{A}$,002$^{-}$000-$\tilde{X}$,000000 of $C_3Ar$ by monitoring the LIF of the type C /A band of $\tilde{A}$,002$^{+}$200-$\tilde{X}$,000000.

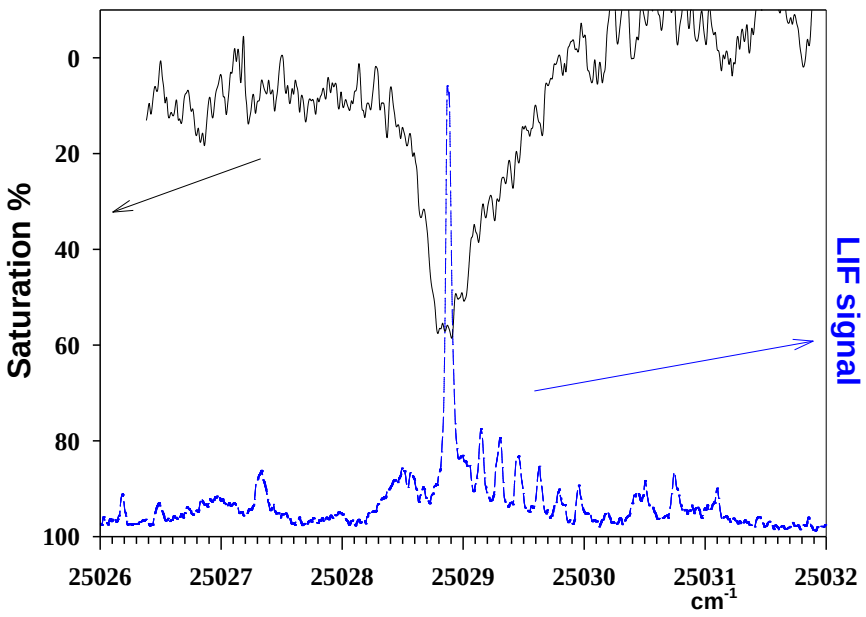


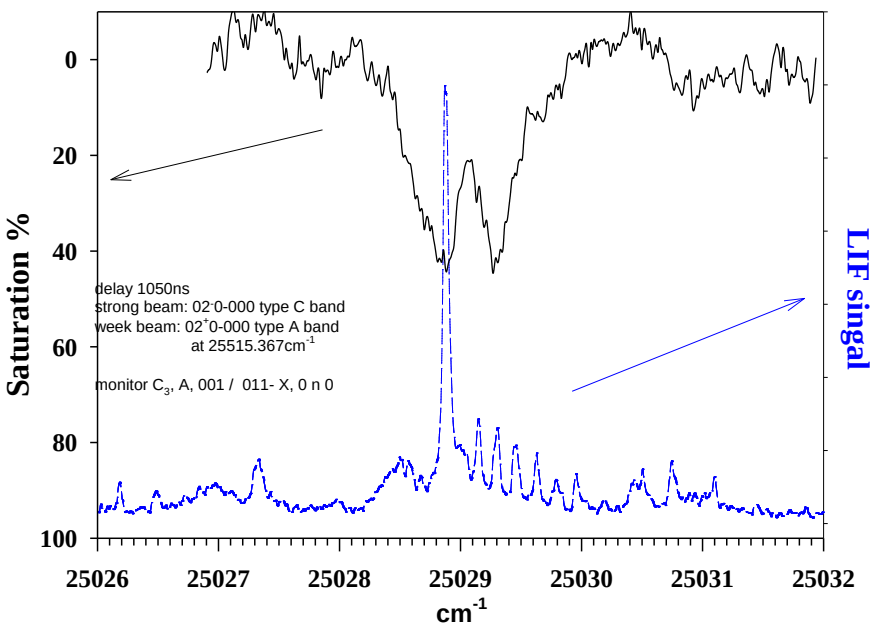


Six rotationally resolvable bands are all excited from the lowest level - - the v=0 of $C_3Ar(\tilde{X})$.

# Higher-resolution UV-UV Hole burning experiment

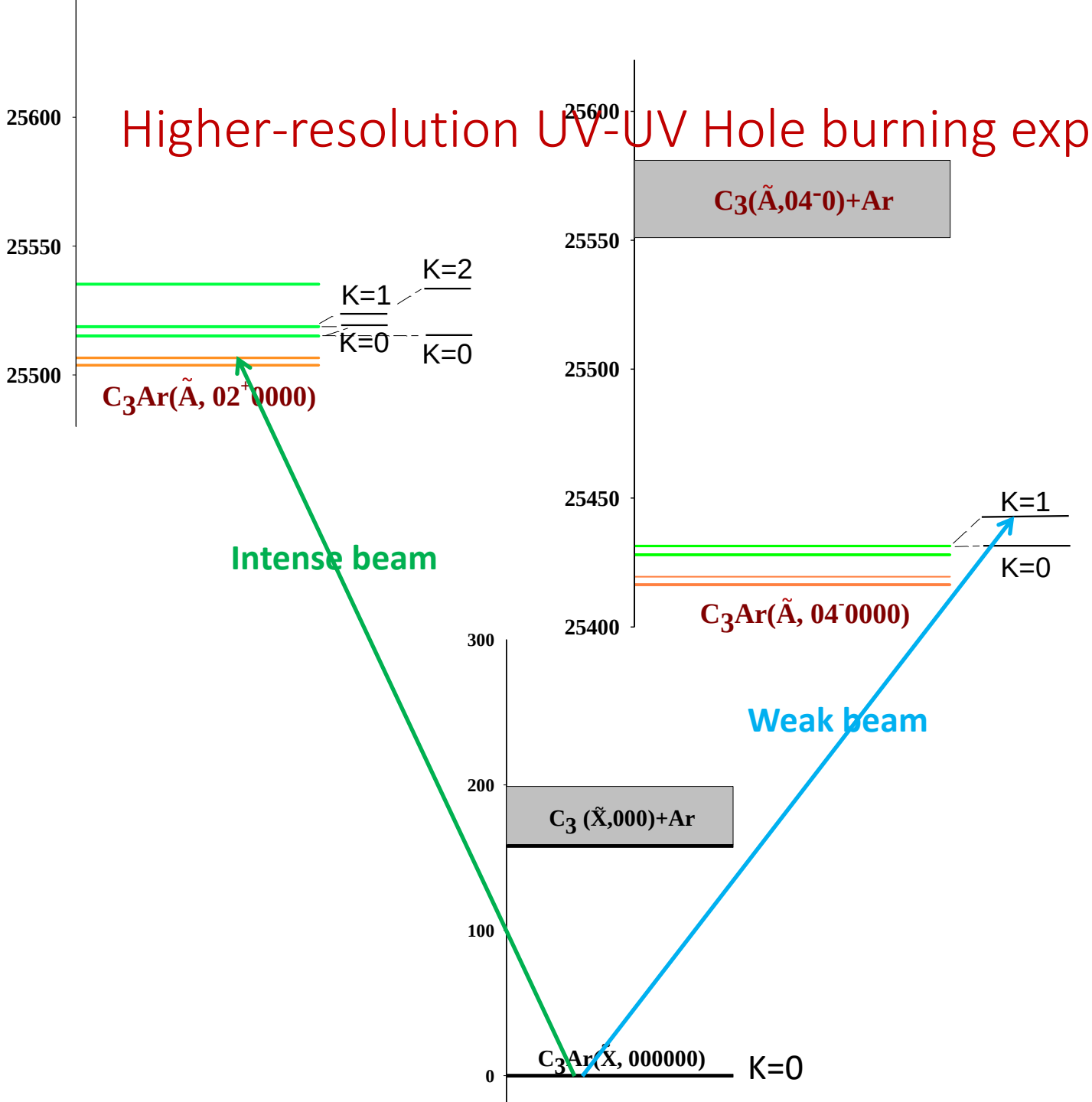

# Hole burning spectrum of the 25506 $cm^{-1}$ band

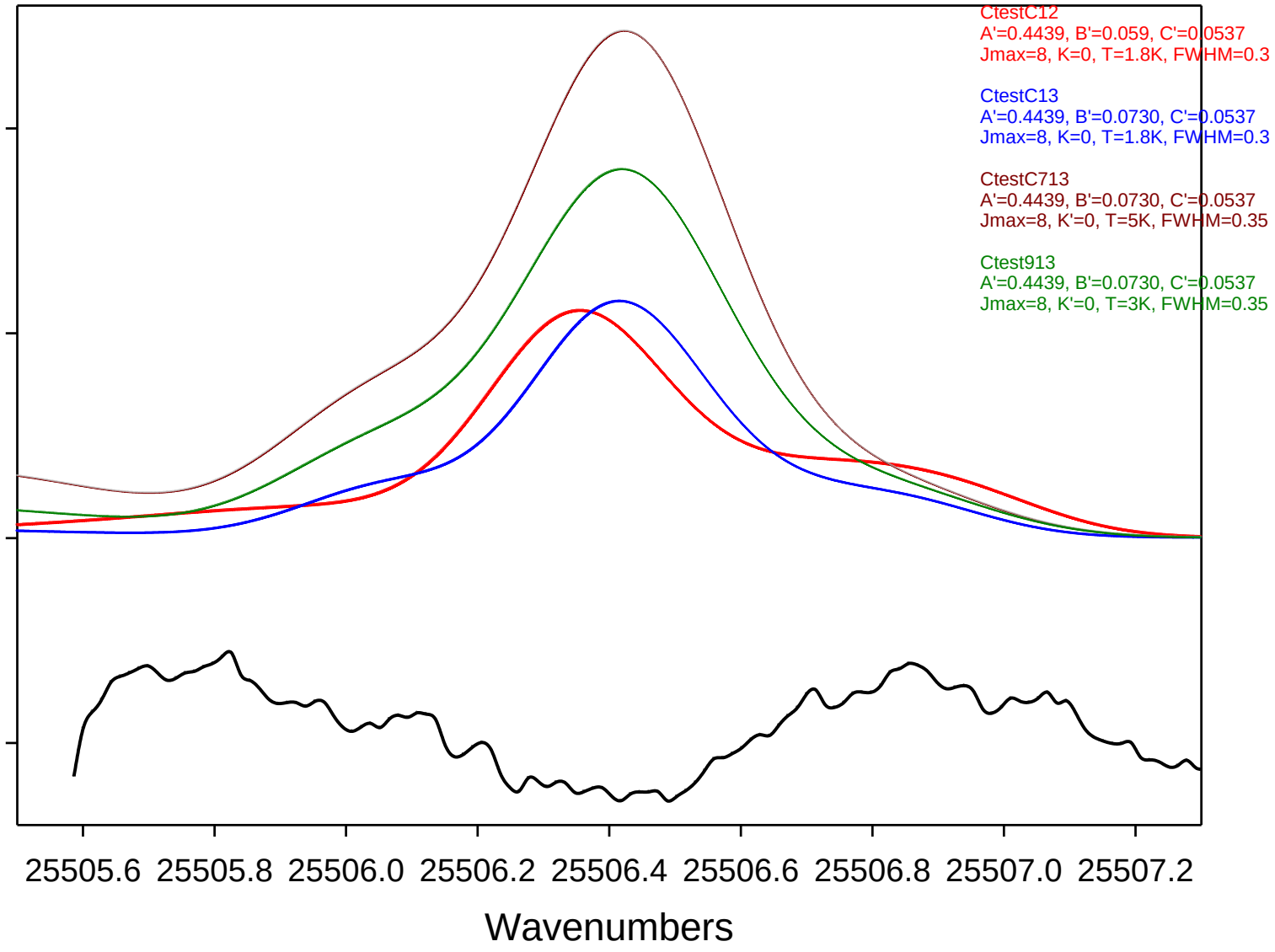

# Hole burning spectrum of the 25504 $cm^{-1}$ band

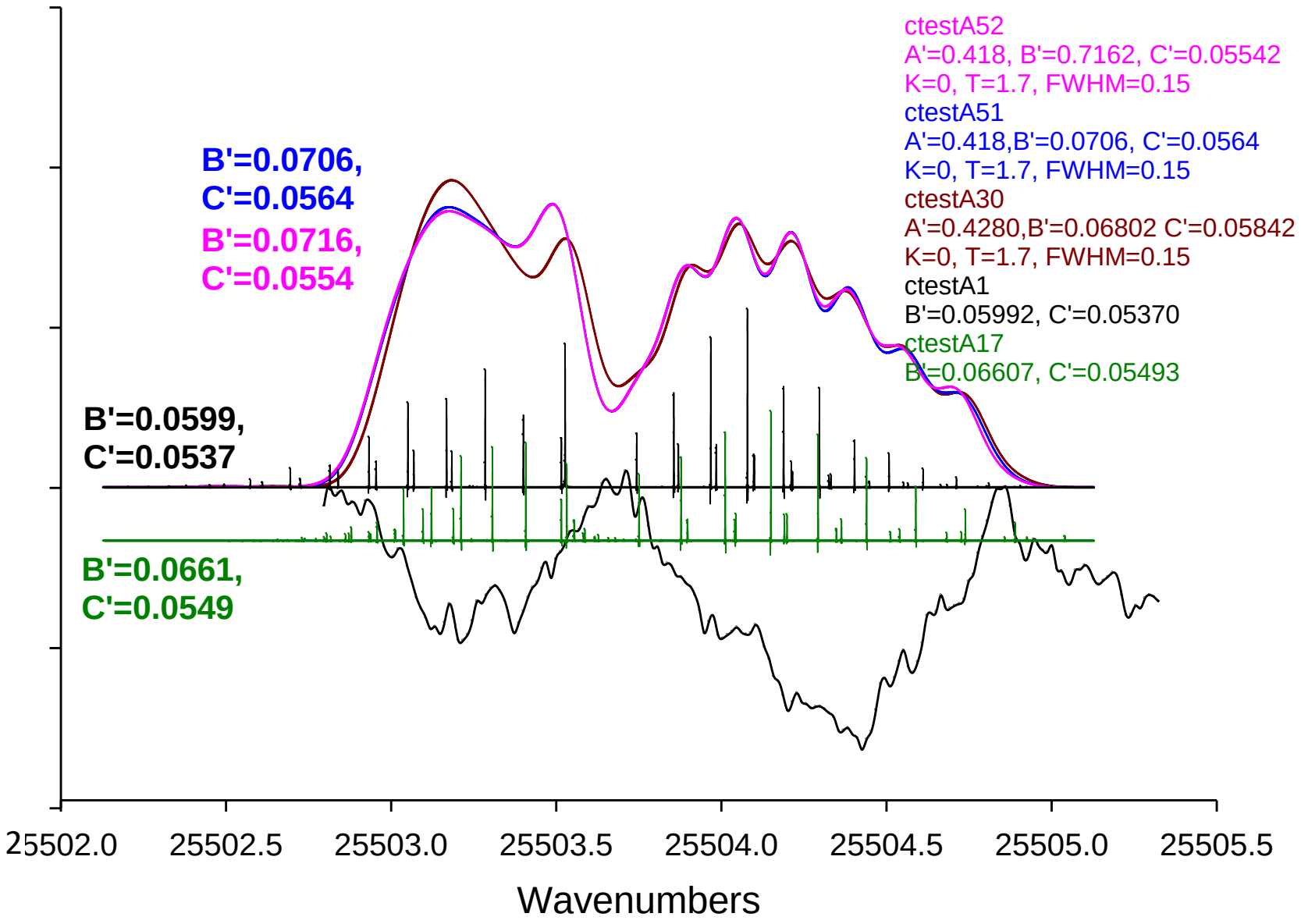

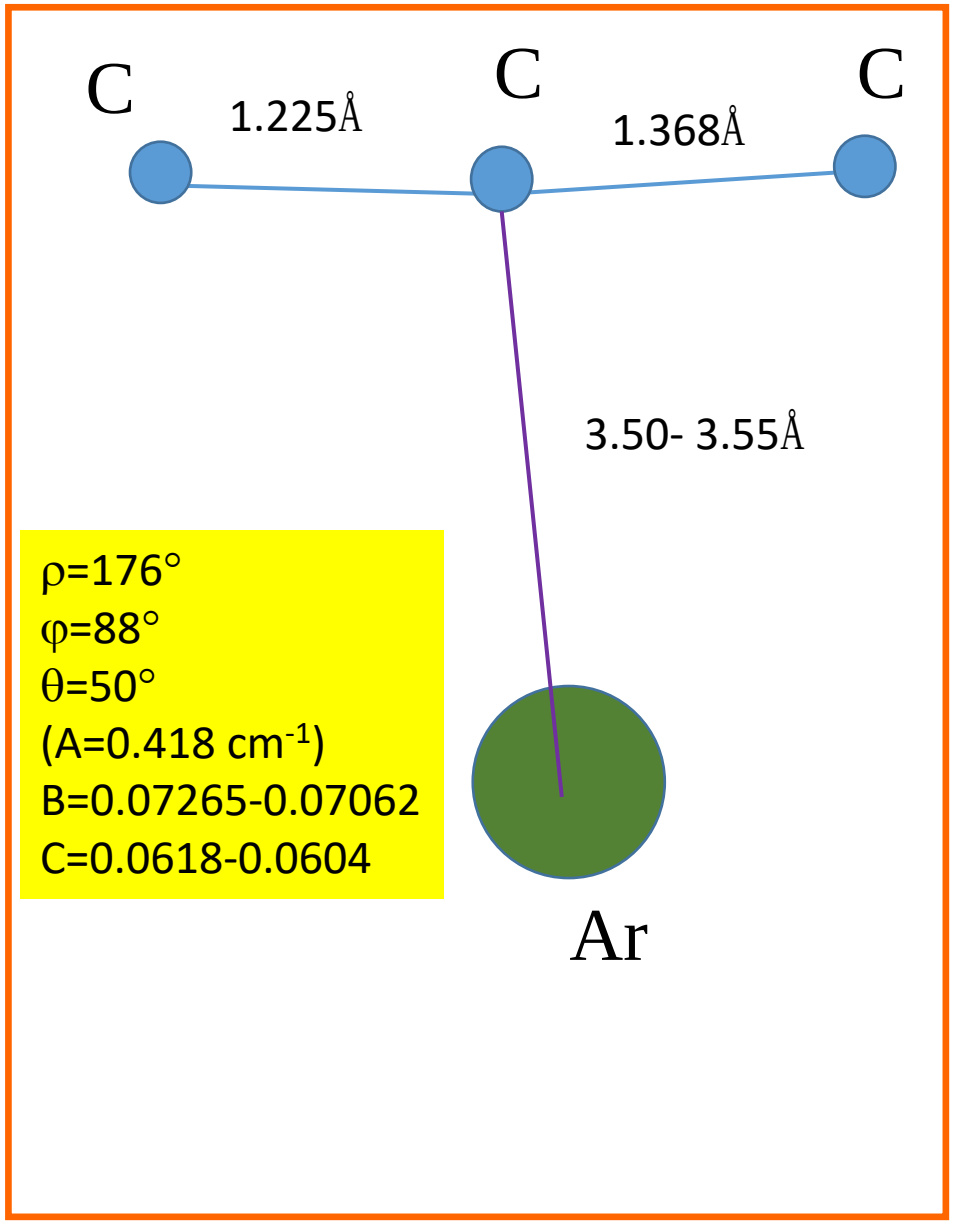
C
1.225Å
C
1.368Å
C
3.50- 3.55Å
ρ=176°
φ=88°
θ=50°
(A=0.418 cm-1)
B=0.07265-0.07062
C=0.0618-0.0604
Ar

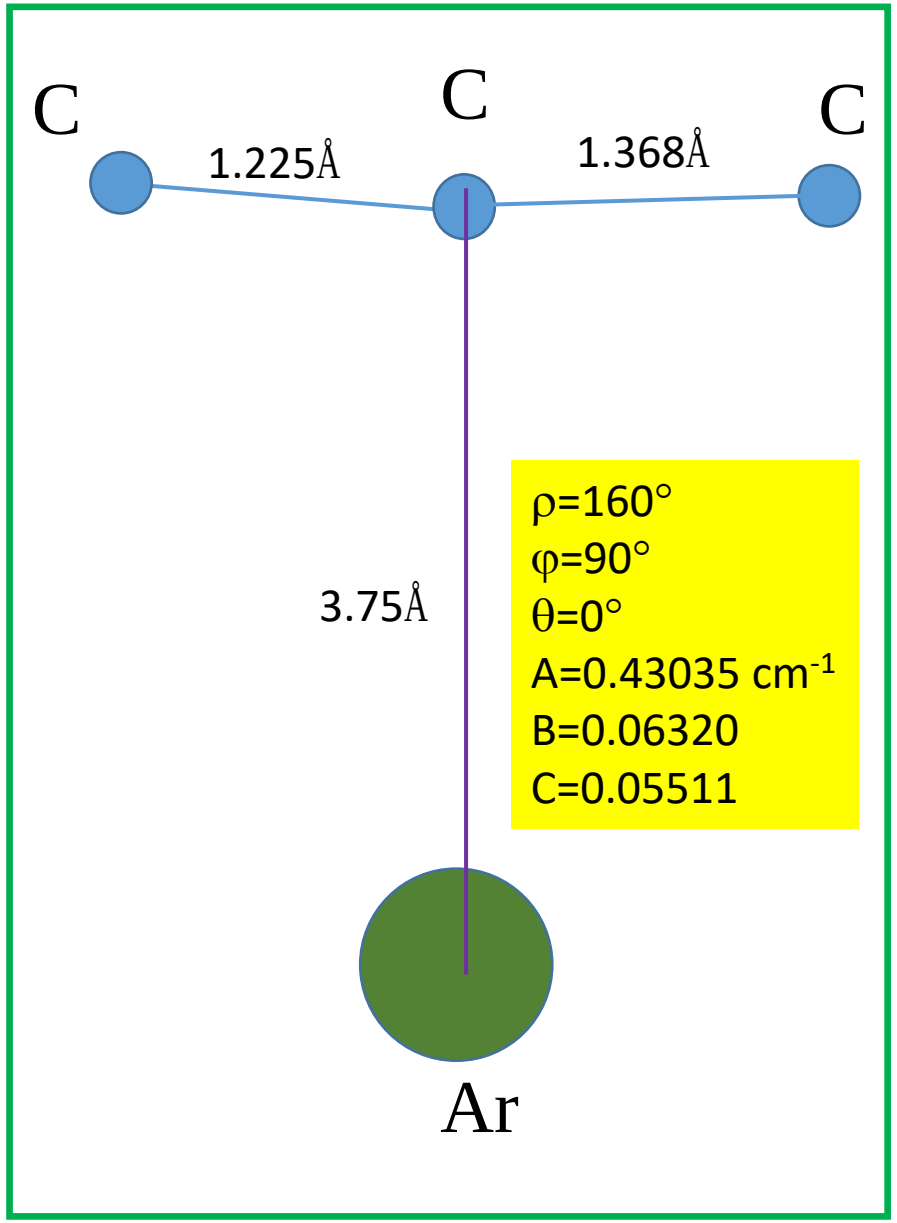
C
1.225Å
C
1.368Å
C
3.75Å
ρ=160°
φ=90°
θ=0°
A=0.43035 cm-1
B=0.06320
C=0.05511
Ar

# *Prospective*

- Studies of the $C_3Ar$ levels which have no $\nu_2'$ excitations.
- Stimulated emission pumping spectrum of the 25431 $cm^{-1}$ band to obtain the internal energy of one of the predissociation products, $C_3$.
- Stimulated emission pumping spectrum of the 26689 $cm^{-1}$ band to obtain the ground state level structure of the $C_3Ar$ complex.

# Acknowledgement

National Central U., Department of Physics

Institute of Atomic and Molecular Sciences
Academia Sinica

Academia Sinica
MOST